



## Calhoun: The NPS Institutional Archive DSpace Repository

---

Theses and Dissertations

1. Thesis and Dissertation Collection, all items

---

1968

### Stabilizing fins for underwater coring tools

Honhart, David Crosby

Monterey, California. Naval Postgraduate School

---

<http://hdl.handle.net/10945/13096>

---

This publication is a work of the U.S. Government as defined in Title 17, United States Code, Section 101. Copyright protection is not available for this work in the United States.

*Downloaded from NPS Archive: Calhoun*



<http://www.nps.edu/library>

Calhoun is the Naval Postgraduate School's public access digital repository for research materials and institutional publications created by the NPS community.

Calhoun is named for Professor of Mathematics Guy K. Calhoun, NPS's first appointed -- and published -- scholarly author.

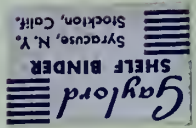
**Dudley Knox Library / Naval Postgraduate School  
411 Dyer Road / 1 University Circle  
Monterey, California USA 93943**

NPS ARCHIVE  
1968  
HONHART, D.

STABILIZING FINS FOR UNDERWATER  
CORING TOOLS

by

David Crosby Honhart



DUDLEY KNOX LIBRARY  
NAVAL POSTGRADUATE SCHOOL  
MONTEREY CA 93943-5101

United States  
Naval Postgraduate School



THE SIS

STABILIZING FINS FOR UNDERWATER

CORING TOOLS

by

David Crosby Honhart

December 1968

*This document has been approved for public release and sale; its distribution is unlimited.*

LIBRARY  
U.S. NAVAL POSTGRADUATE SCHOOL  
MONTEREY, CALIFORNIA

STABILIZING FINS FOR UNDERWATER CORING TOOLS

by

David Crosby Honhart  
Lieutenant, United States Navy  
B. S., Naval Academy, 1963

Submitted in partial fulfillment of the  
requirements for the degree of

MASTER OF SCIENCE IN OCEANOGRAPHY

from the

NAVAL POSTGRADUATE SCHOOL  
December 1968

NPS ARCHIVE

1968

HONHART, D.

~~Thesis~~  
~~H 919~~  
~~8.2~~

## ABSTRACT

It is essential that the force vector of the weight of a coring tool act along a line that is parallel to the longitudinal axis of the core barrel. Such an alignment enables corers to obtain deeper, less disturbed core samples. The probability of bending the core barrel is furthermore greatly reduced. A fin assembly that provides the maximum righting moment for one shape of coring tool does not necessarily provide the maximum moment for a different shape. The optimum fin design is determined by testing. A fin assembly for a particular coring tool has been devised which reduces the probability of the force vector not acting parallel to the longitudinal axis. The optimum design is a vane-shroud fin assembly. The shape of the shroud is conical. Slotting the shroud by removing longitudinal strips improves the righting capability at higher angles of deviation, but is slightly inferior to the full shroud at lesser angles.

TABLE OF CONTENTS

	<u>Page</u>
A. INTRODUCTION	13
B. WIND TUNNEL TESTING	15
1. <u>Modeling</u>	17
2. <u>Test Equipment</u>	17
3. <u>Procedure</u>	21
4. <u>Tests</u>	24
5. <u>Test Data Reduction</u>	26
C. RESULTS AND DISCUSSION	34
D. SUMMARY COMMENTS	46
REFERENCES	48
APPENDIX	49



LIST OF TABLES

<u>Table</u>		<u>Page</u>
1.	Tabulated data of adjusted moment, temperature, air speed, and drag coefficient for coring tool model without fins	32
2.	Comparison of model drag and drag coefficient for fins 3, 4, 5, and 6, reversed and regular	45
A-V	Tabulated data of adjusted moment, temperature, air speed, and drag coefficient for coring tool model with various fin assemblies	50-71
W	Reynolds number and drag coefficient, calculated for variable wind speed at constant angle of deviation	72



LIST OF FIGURES

<u>Figure</u>		<u>Page</u>
1.	Angle of Deviation "vs" Righting Moment coring tool model (without fins)	36
2.	Angle of Deviation "vs" Righting Moment coring tool model (fin 1)	37
3.	Angle of Deviation "vs" Righting Moment coring tool model (fin 2)	38
4.	Angle of Deviation "vs" Righting Moment coring tool model (fin 3)	39
5.	Angle of Deviation "vs" Righting Moment coring tool model (fin 4)	40
6.	Angle of Deviation "vs" Righting Moment coring tool model (fin 5)	41
7.	Angle of Deviation "vs" Righting Moment coring tool model (fin 6)	42
8.	Angle of Deviation "vs" Righting Moment coring tool model (fin comparison)	43
9.	Drag Coefficient "vs" Reynolds Number	44



LIST OF PLATES

<u>Plate</u>		<u>Page</u>
1.	Coring tool model with support rods	18
2.	Coring tool model assembled with fin	19
3.	Fin assemblies	20
4.	Schematic-horizontal wind tunnel	22
5.	Aerolab 3 component beam balance	23
6-9.	Photographs of various coring tool-fin assemblies	27-30



### NOMENCLATURE AND SYMBOLS

Alignment:	refers to vane orientation about the longitudinal axis of the model with respect to horizontal and vertical
Angle of Deviation:	( $\alpha$ ), measured in the vertical in degrees
Fin Assembly:	consisting of four vanes with or without exterior shroud
Inferior:	refers to having less righting moment
Pitch:	to deviate from a line of sight by angular motion about the transverse horizontal axis of the model
Range:	refers to the range of the angle of deviation, $0^\circ$ to $35^\circ$ through which testing was conducted
Righting Moment:	(-) moment infers a return to vertical descent (+) moment infers turning away from vertical descent
Separation Distance:	minimum distance from the rear of the driving weight to the most forward part of the fin
Shroud:	exterior covering over the vanes
Superior:	refers to better righting moment
Type:	Regular (reg.), tapered edge (leading edge) of vanes is pointed toward the driving weight Reversed (rev.), tapered edge of vanes is pointed away from the driving weight Modified (mod.), exterior shroud is cut back to the point of intersection of vane and shroud Slotted (slo.), longitudinal strips are cut and removed from the shroud. The width of a strip is approximately $1/8$ of the shroud circumference. Four strips were removed from each fin assembly
Vanes:	flat extended surface attached parallel to the longitudinal axis of the coring tool model
Yaw:	to deviate from a line of sight by angular motion about the transverse vertical axis

#### ACKNOWLEDGMENTS

A sincere debt of gratitude is owed to Dr. R. J. Smith of the Department of Oceanography and Dr. D. C. Wooten of the Department of Aeronautics who offered their time, talent, suggestions and encouragement, without whose help the successful completion of this thesis perhaps would not be a reality, to Mr. N. Walker and Mr. G. Smith of the Machine Facility who did an excellent job of constructing the model, and to Mr. W. S. Johnson of the Aeronautics Laboratory who was kind enough to help with the testing phase.

## INTRODUCTION

There is a variance of opinion as to the necessity of having stabilizing fins on underwater sediment coring tools. This diversity can be attributed to the general lack of research on the subject of coring tool stabilization, as is evidenced by the sparsity of prior information.

According to Rosfelder (1966) the main present concern in short core sampling is to obtain an undisturbed sample. The combination of slow, steady penetration rate and a minimum entry angle on the core cutter achieves this goal. Minimum entry angle and the greatest depth penetration are simultaneously achieved by a coring tool that has the force vector of its total weight acting parallel to the longitudinal axis of the core barrel. Should the force vector deviate from this ideal trend by any angular amount, the depth of penetration will be reduced, the disturbance of the sample increased, and the probability of bending the core barrel increases. One method of obtaining slow, steady penetration is with the use of a high drag, high stability fin assembly.

Free fall coring tools without fins seek to orient themselves so as to fall on their sides when offset the slightest amount from a vertical descent. The majority of all coring tools are lowered on wires. Because of the tension maintained on the wire during lowering, the coring tool is held upright during its entire descent. The coring tools that do not experience a free fall phase during its descent may not require fin stabilization.

Hvorslev (1949) states that the energy available to force a gravity coring tube into the bottom sediments is composed of the static energy or weight of the coring tool, and of the kinetic energy or velocity of the tool as it reaches the bottom. Hvorslev further noted that additional energy and velocity can be obtained by attaching the coring tool to the

cable in such a manner that it is released at a predetermined distance from the bottom, and then allowed to fall freely through the water. The probability that a coring tool without fins will become offset from the vertical increases with the height of release.

The foregoing indicates the desirability for a fin type device that will provide the greatest amount of righting moment to insure a return to the vertical descent as quickly as possible. The subject of this investigation has been to study the relative righting moment of various fin assemblies.

## 2. WIND TUNNEL TESTING

One means of measuring the moment and drag characteristics of various fin assemblies is to make scale models of the fins, and by use of a wind tunnel and its associated equipment to make the necessary measurements. According to Pope (1966) wind tunnels should be used because they provide a rapid, economical and accurate means for aerodynamic research. Ohart (1946) and Poston (1948) state that the optimum fin design for a particular shaped body can be determined only from testing. It is possible to calculate the moment and drag of fin assemblies and body shapes from theory. However the difficulty of obtaining an accurate result increases with the complexity of the fin assembly - body shape, and solutions to complex fin-body combinations are not easily attained.

Meaningful wind tunnel modeling is dependent upon simulating the conditions of flow in the fluid field in which the actual coring will occur. This requires the matching of the Reynolds Number and the Mach Number.

Two flow systems are considered by Streeter (1958) to be dynamically similar when corresponding linear dimensions have a constant ratio, and pressure intensities at corresponding points have a constant ratio. Reynolds deduced that two flow situations would be dynamically similar if the general differential equation describing their flow were identical. By changing the values of length, time, and mass in one set of equations and then determining the conditions that must be satisfied to make them identical to the original equations, Reynolds found that the dimensionless group

$$\frac{u \rho}{\mu} l$$

$u$  = speed of flow  
 $l$  = characteristic dimension  
 $\rho$  = density of the medium  
 $\mu$  = dynamic viscosity

must be the same for both flows.

The approach used is to solve for a Reynolds number representative of a coring tool descending in water, and then to calculate the wind tunnel air speed necessary to match that Reynolds number.

The choice of cross-sectional dimension to use as the characteristic dimension is unimportant since a constant ratio exists between the dimensions of the actual coring tool and the model. The same air speed will be calculated regardless of the dimension used, provided that the dimensions are of similar parts of the tool and model, (as for instance the driving weights).

Hvorslev (1949) states that the safe unreeling speed of a winch and therefore the downward velocity of a gravity coring tool is normally between 3 and 10 feet per second (fps). To compute the Reynolds number an average speed of 6.5 fps was used. The cross-sectional dimension of the driving weight of the actual corer, 1.187 ft, was chosen as the characteristic dimension. The density of a representative sample of sea water with a salinity of 35°/00, a temperature of 20°C, and at atmospheric pressure is  $1.989 \text{ slug ft}^{-3}$ . The dynamic viscosity for the same conditions of temperature, salinity, and pressure is  $2.28 \times 10^{-5} \text{ slug ft sec.}$  These values resulted in a Reynolds number of 674461. The corresponding wind tunnel air speed using the dimension of the model driving weight of 0.247 ft as the characteristic dimension was 457.6 fps, which converts to 312 mph. This exceeds the 200 mph rated upper limit of the wind tunnel used. However the corresponding speed of descent for the ocean using 200 mph is 4.36 fps, which is well within the estimated coring tool descent speed limits. The air speed in the tunnel varied during testing between 207 and 190 mph. Therefore the testing at all times simulated speeds of descent in salt water between 4.14 and 4.51 fps. Pope (1966) indicates that the Mach number ( $N_m$ ) effects are rarely important for values less

than 0.4.  $N_m$  for 200 mph is 0.266.

Another factor which must be considered is the nature of the compressibility of the fluids, sea water and air. Schlichting (1960) states that the compressibility of a gas can be ignored if  $0.5 N_m^2$  is much less than 1. This value for 200 mph is 0.0357. Streeter (1958) states that fluid flow may be treated as incompressible if the density changes are gradual and do not vary by more than a few percent.

## 1. MODELING

A corer presently manufactured and extensively used was selected and an approximate 1:4.8 scale model of it was made out of solid stock aluminum. The driving weight and core barrel are one piece, bored through along the longitudinal axis and tapped at the trailing end. Various fin assemblies were fabricated which could be mounted on the trailing end. They were separated from the driving weight by various length sleeves, locked in place to prevent backing off by a stud and lock nut. The total length of the finished model was 20 inches, 10 inches of which is core barrel (Plates 1 and 2).

In order to make some aspects of the different fin assemblies somewhat comparable, various dimensions were maintained as constants. The height of all fin assemblies is the same. The minimum exterior diameter of fins 2 through 6 is the same dimension as the largest diameter of fin 1 (Plate 3). The interior vanes of fins 2 through 6 have the same leading edge angle as that of fin 1.

## 2. TEST EQUIPMENT

The U. S. Naval Postgraduate School Aerolab 32 x 45 inch sub-sonic, atmospheric wind tunnel is a continuous operating, closed circuit wind tunnel having a speed range of 0 to 200 mph (Plate 4).

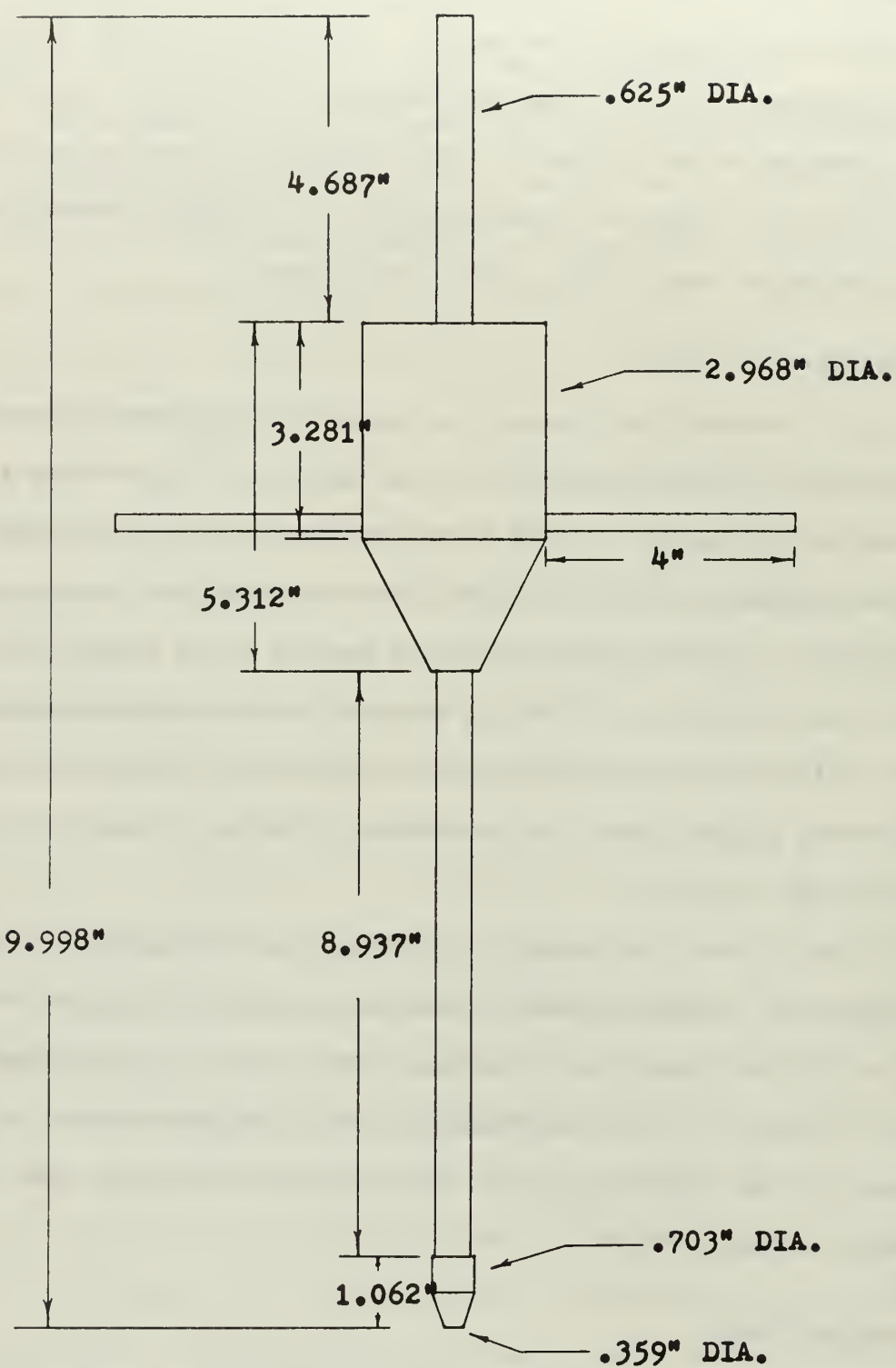
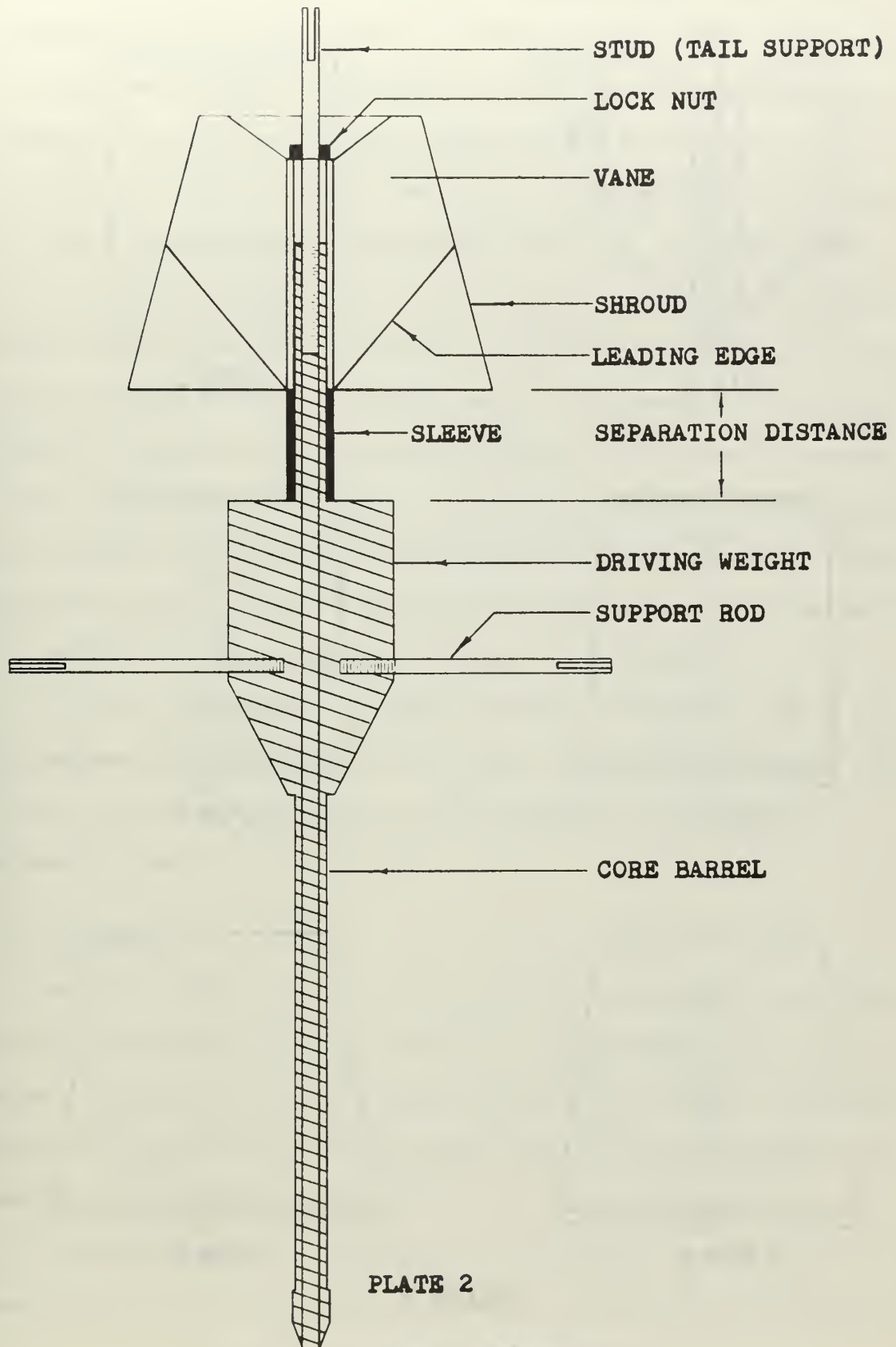
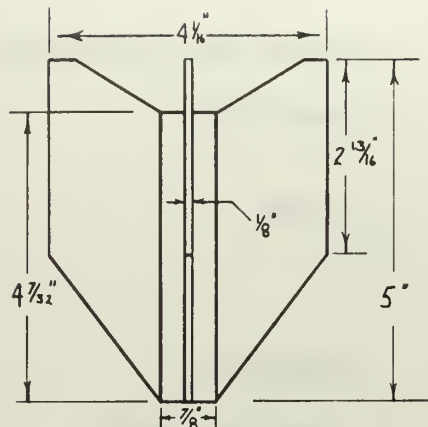


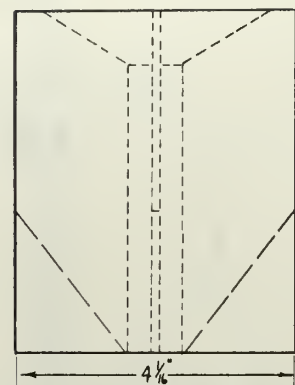
PLATE 1

Coring Tool Model with Support Rods

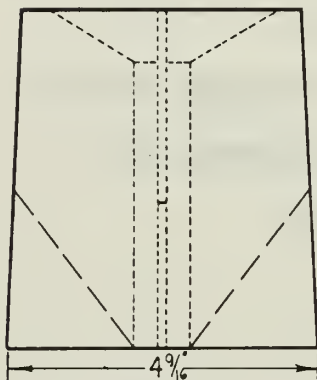




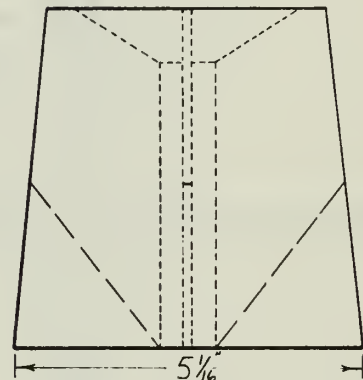
**FIN 1**



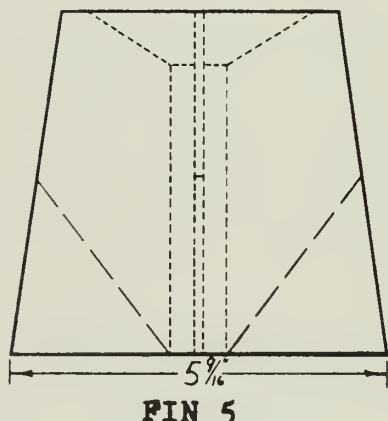
**FIN 2**



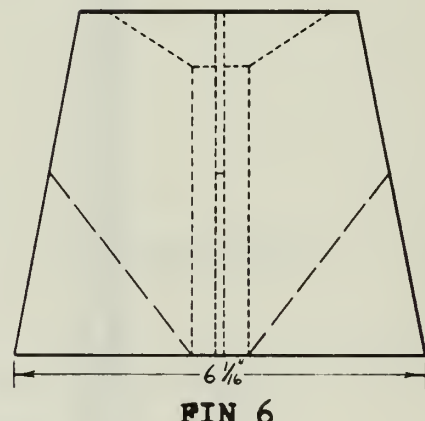
**FIN 3**



**FIN 4**



**FIN 5**



**FIN 6**

**PLATE 3**

### **Fin Assemblies**

The Aerolab "543" wind tunnel beam balance contains three essentially separate force measurement systems combined into one.

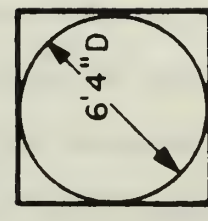
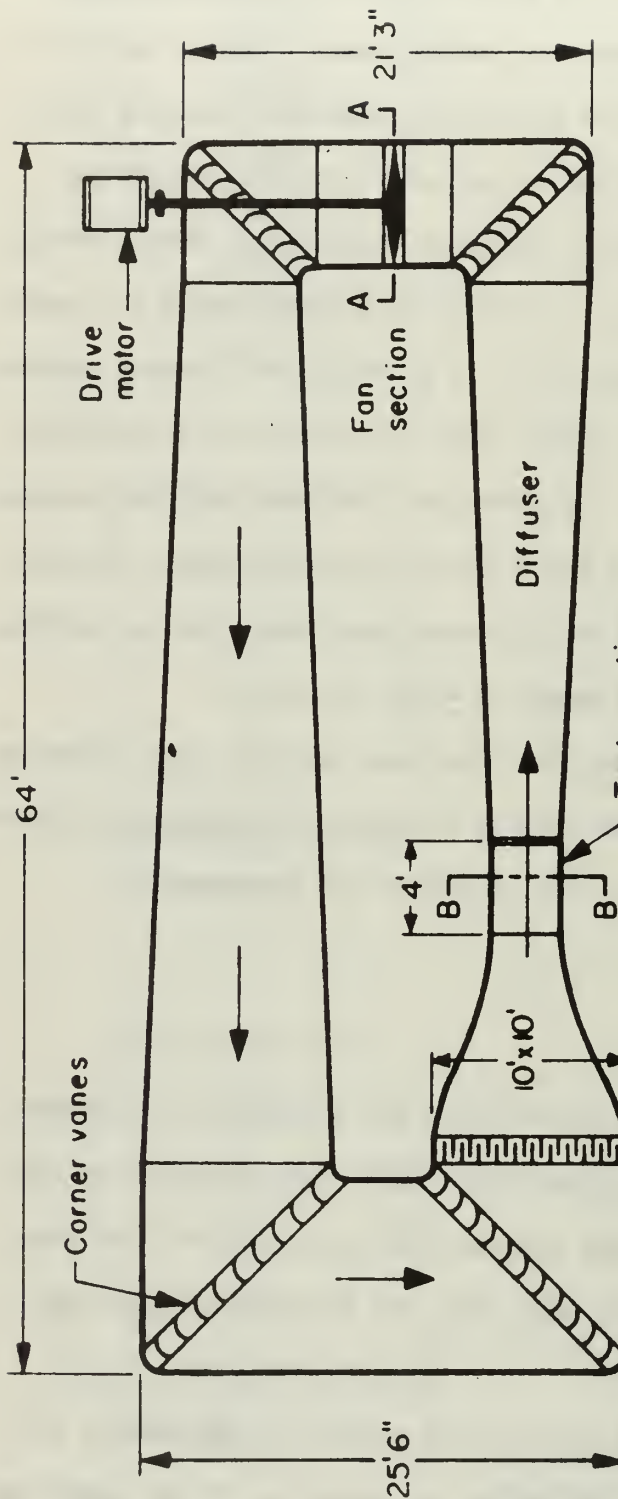
The model is supported by means of three struts. Two wing struts restrain the model against lift, drag and yawing moment forces, and the tail strut restrains pitching moments about the wing strut holding pins. Each force and moment measuring system is entirely independent and is balanced singly. The gross forces are measured by manually manipulating weights, large values being measured on graduated notched beams and small values measured by means of a weight moved on a graduated threaded spindle. Balance is indicated when two neon lights that are actuated by sensitive contact points flicker uniformly. The beams are equipped with adjustments for balancing out the weight of the model and zeroing the beams, thereby permitting data to be read from an initial zero position. During testing the model may be pitched through a range of  $\pm 45^\circ$  (Plate 5).

Air speed calculations are made from the data recorded from a 100 cm micromanometer. Temperature is read from a bimetallic thermometer located in the tunnel wall. Calibration of all equipment was performed by Aeronautics Laboratory technicians.

### 3. PROCEDURE

The desired fin - coring tool combination was assembled and mounted on to the beam balance struts using metallic dowel pins, insuring in the process that the model was not bound and was free to rotate on the pins. The model alignment was checked for zero yaw, and the beam balance yaw indicator was adjusted accordingly.

A portable mechanical angle indicator was placed on the model, to determine the correlation between the angle of deviation of the model and



Section A-A



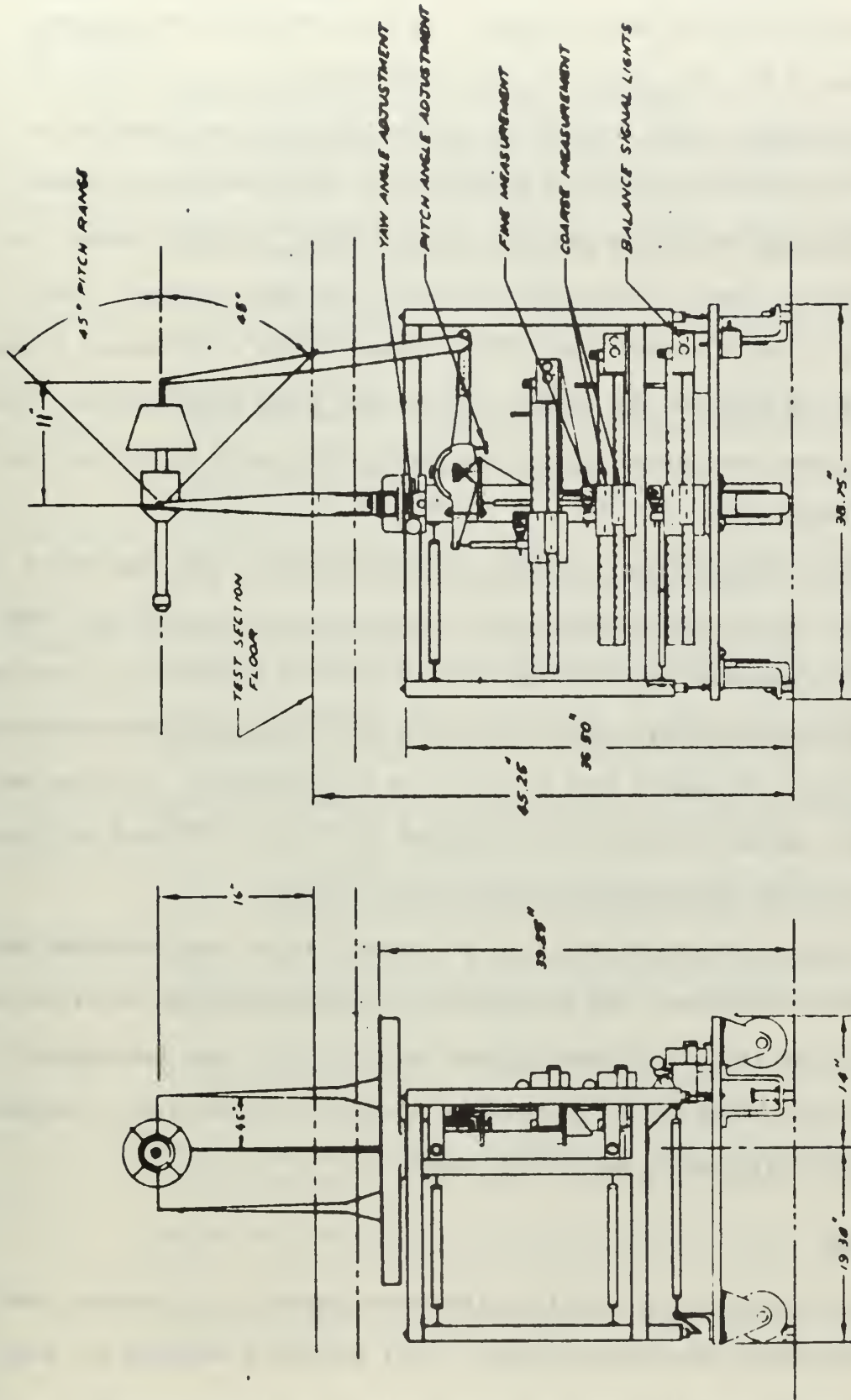
Section B-B

PLATE 4

SCHEMATIC - HORIZONTAL WIND TUNNEL

AEROLAB 3 COMPONENT BEAM BALANCE

PLATE 5



the beam balance pitch indicator. The beam balance pitch indicator was adjusted until the portable indicated zero angle. The angle indicated by the pitch indicator was recorded. The same procedure was followed for angles of  $5^\circ$ ,  $10^\circ$ ,  $15^\circ$ ,  $20^\circ$ ,  $25^\circ$ ,  $30^\circ$ , and  $35^\circ$ .

The vibrator motor attached to the beam balance was turned on to eliminate static friction while balancing the force measuring systems. After balancing the moment and drag force systems, the tare moment for each assembled model was measured at each of the above angles. Tare moment is a static moment that exists because of the distribution of the weight of the model on the struts with no wind force being applied. The vibrator motor was turned off and the wind tunnel motor started and run up to maximum rpm.

With the balance pitch indicator adjusted to  $0^\circ$ , the temperature and the height of the micromanometer were recorded and the moment and drag forces were measured by balancing their respective systems until the neon lights flickered evenly. After recording the  $0^\circ$  values, measurements were also made for the angles from  $5^\circ$  to  $35^\circ$  in  $5^\circ$  increments. Prior to measuring the moment and drag for the angles of  $0^\circ$ ,  $10^\circ$ ,  $20^\circ$ , and  $30^\circ$ , the temperature and micromanometer height were recorded.

On various occasions the drag and moment values were rechecked prior to stopping the motor. Due to the rise in temperature that occurred with each run, the last significant figure would vary for each measurement. However this change was of a magnitude at most of a few digits, and was therefore considered to be insignificant.

#### 4. TESTS

The effects of fin rotation, sleeve separation, fin reversal, and fin modification were investigated. Fin 1 and fin 2 modified are similar to fin types presently used on coring tools. The righting moment of these

fins was established through testing and compared against the righting moment of fins 3 through 6.

Run Number

1. Coring tool model with no fins attached
2. Coring tool model, fin 1 attached, 1 inch sleeve separation, vanes oriented in a horizontal/vertical position (+)
3. Coring tool model, fin 1 attached, 1 inch sleeve separation, vanes oriented 45 degrees from position in run 2 (X)
4. Coring tool model, fin 2 attached, 1 inch sleeve separation, vanes oriented in a horizontal/vertical position (Plate 6)
5. Coring tool model, fin 3 attached, 1 inch sleeve separation, vanes oriented in a horizontal/vertical position, regular type
6. Coring tool model, fin 3 attached, 1 inch sleeve separation, vanes oriented 45 degrees from position in run 5, regular type
7. Coring tool model, fin 4 attached, 1 inch sleeve separation, vanes oriented in a horizontal/vertical position, regular type
8. Coring tool model, fin 5 attached, 1 inch sleeve separation, vanes oriented in a horizontal/vertical position, regular type
9. Coring tool model, fin 6 attached, 1 inch sleeve separation, vanes oriented in a horizontal/vertical position, regular type
10. Coring tool model, fin 3 attached, 1.25 inch sleeve separation, vanes oriented in a horizontal/vertical position, reversed type
11. Coring tool model, fin 4 attached, 1.25 inch sleeve separation, vanes oriented in a horizontal/vertical position, reversed type
12. Coring tool model, fin 5 attached, 1.25 inch sleeve separation, vanes oriented in a horizontal/vertical position, reversed type (Plate 8)
13. Coring tool model, fin 6 attached, 1.25 inch sleeve separation, vanes oriented in a horizontal/vertical position, reversed type
14. Coring tool model, fin 1 attached, 2 inch sleeve separation, vanes oriented in a horizontal/vertical position (Plate 6)
15. Coring tool model, fin 2 attached, 2 inch sleeve separation, vanes oriented in a horizontal/vertical position
16. Coring tool model, fin 5 attached, 2 inch sleeve separation, vanes oriented in a horizontal/vertical position, regular type

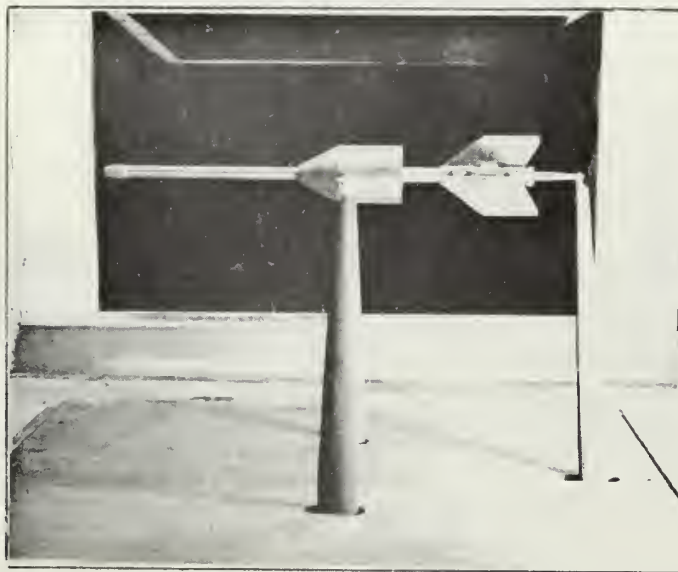
Run Number

17. Coring tool model, fin 2 attached, 2 inch sleeve separation, vanes oriented in a horizontal/vertical position, modified type (Plate 7)
18. Coring tool model, fin 5 attached, 2 inch sleeve separation, vanes oriented in a horizontal/vertical position, modified type
19. Coring tool model, fin 6 attached, 2 inch sleeve separation, vanes oriented in a horizontal/vertical position, modified type (Plate 9)
20. Coring tool model, fin 5 attached, 2 inch sleeve separation, vanes oriented in a horizontal/vertical position, modified-slotted type
21. Coring tool model, fin 5 attached, 1.25 inch sleeve separation, vanes oriented in a horizontal/vertical position, reversed-modified-slotted type (Plate 9)
22. Coring tool model, fin 4 attached, 1.25 inch sleeve separation, vanes oriented in a horizontal/vertical position, reversed-slotted type
23. Coring tool model, fin 4 attached, 1.25 inch sleeve separation, vanes oriented 45 degrees from position in run 22, reversed-slotted (Plate 8)
24. Beam balance struts without model attached, to determine drag contributed by struts at zero angle of deviation
25. Coring tool model with no fins attached, zero angle of deviation, air speed increased from 60 to 200 miles per hour at 5 centimeter increments. The purpose was to obtain data to plot drag coefficient versus Reynolds number
26. Coring tool model, fin 6 attached, 2 inch sleeve separation, vanes oriented in a horizontal/vertical position, modified-slotted type, same testing procedure as run 25

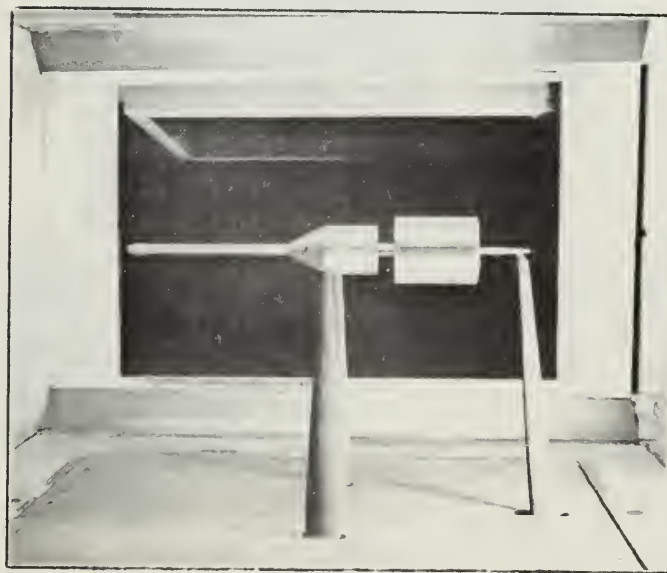
5. TEST DATA REDUCTION

Gross moment is the quantity registered by the beam balance. From this value the tare moment is subtracted, to yield the net righting moment. Since the model is theoretically symmetrical in all respects, there should be no net moment at  $0^\circ$  angle of deviation. Values registered at  $0^\circ$  were likely caused in part by the support rods which attached the model to the

PLATE 6



FIN 1:      separation: 2 in.  
                 alignment: +  
                 type:      reg.



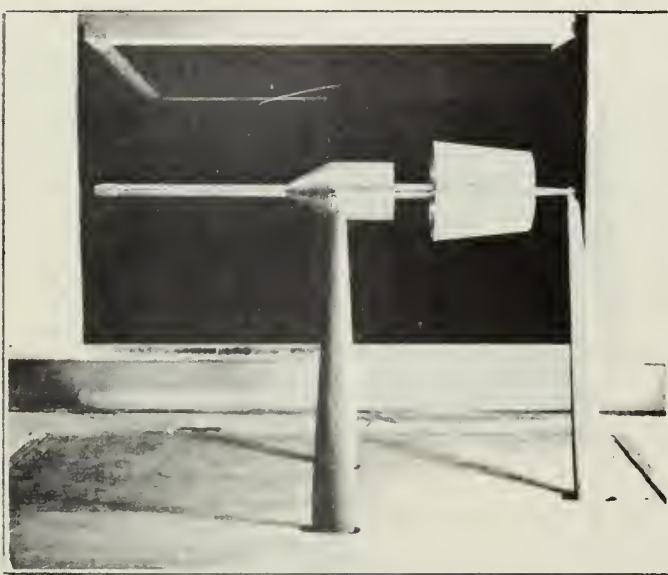
FIN 2:      separation: 1 in.  
                 alignment: +  
                 type:      reg.



PLATE 7



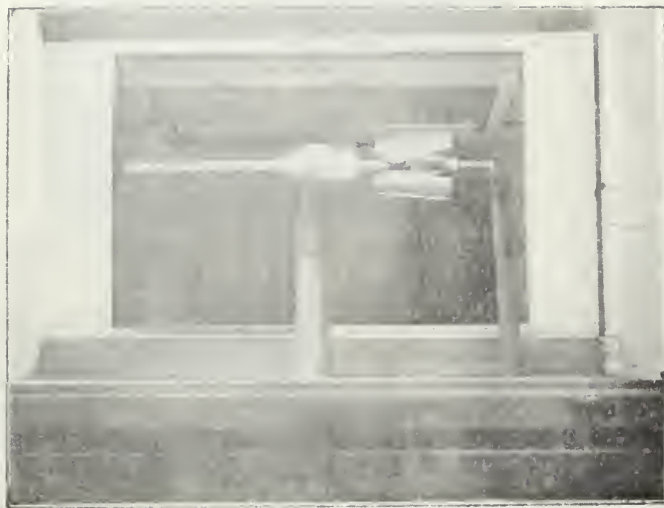
FIN 2: separation: 2 in.  
alignment: +  
type: mod.



FIN 4: separation: 2 in.  
alignment: +  
type: reg.

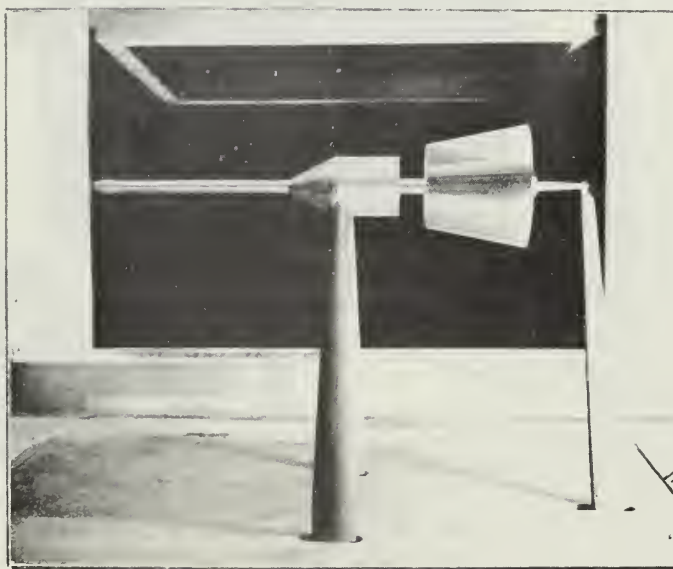


PLATE 8



FIN 4

separation: 1.25 in.  
alignment: X  
type: rev. slo.

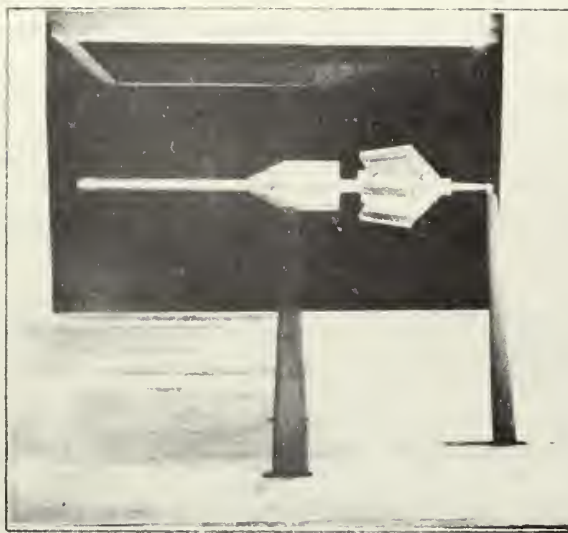


FIN 5:

separation: 1.25 in.  
alignment: +  
type: rev.



PLATE 9



FIN 5

separation: 1.25 in.  
alignment: +  
type: rev. mod. slo.



FIN 6 :

separation: 2 in.  
alignment: +  
type: mod.



balance struts and in part by minor warping of the vanes during welding.

To obtain a zero net righting moment at 0°, the moment at 0° was subtracted from each of the values for 0° through 35° (Table 1).

The wind tunnel air speed as measured by the calibrated Pitot tube in the "543" tunnel was calculated from the empirical relationship for that Pitot tube using the micromanometer reading as follows:

$$V = 28.26 \sqrt{h}$$

V = wind tunnel air speed (mph)  
h = micromanometer fluid height (cm)

The gross drag is that quantity registered by the balance. From this value the drag due to the balance struts was subtracted, yielding the model drag (Table 1). Fin drag is the result of subtracting the model drag without fins from the model drag of the tool-fin combination being investigated. This drag is the drag contributed by the fin for that particular combination, and is not the total drag of the fin assembly that would be recorded if the fin assembly was tested unattached to a coring tool.

Drag coefficient,  $C_D$ , was calculated using the value of model drag.

$$C_D = \frac{2 D}{A \rho u^2}$$

$\rho$  = density of the gas  
A = cross sectional area computed using the characteristic diameter  
u = air speed  
D = model drag

In determining the coefficient of drag from wind tunnel experimentation, the effect of drag caused by the tunnel walls should be considered. Since this study was a determination of the relative performance of various fin assemblies, it was not considered essential to determine the wall drag effect. Any deficiency in the calculated data should be small since the

TABLE 1

CORING MODEL (No Fins)

Type: NA

Separation: NA

Alignment: NA

$\alpha_{bal.}$	$\alpha$	gross moment in lbs.	tare moment in lbs.	net moment in lbs.	adjusted moment in lbs.	temp. °F	cm. $H_2O$	speed m.p.h.
+ 30°	0	-1.78	0	-1.78	0	83	50.44	200.70
+ 5°50'	5	-.54	-.27	-.27	+ 1.51			
+ 11°	10	-.59	-0.78	+.19	+ 1.97			
+16°10'	15	-1.07	-1.42	+.35	+ 2.13			
+21°15'	20	-.30	-2.32	+2.30	+ 4.08			
+26°35'	25	+1.19	-3.36	+4.55	+ 6.33			
+31°50'	30	+2.15	-4.61	+6.76	+ 8.54			
+37°20'	35	+2.20	-6.05	+8.25	+10.03	90	47.87	195.52

$\alpha$	gross drag lbs.	support drag lbs.	model drag lbs.	fin drag lbs.	$C_D$
0	+5.491	+2.598	+2.893	NA	.579
5	+5.792				
10	+6.025				
15	+6.475				
20	+7.265				
25	+7.598				
30	+8.350				
35	+8.774				

model was small compared to the tunnel test section. Net righting moment, drag coefficient, temperature, and air speed data are recorded in Appendix Tables A through V. The data for runs 25 and 26 is recorded in Appendix Table W.

## RESULTS AND DISCUSSION

Righting moment versus angle of deviation for runs 1 through 23 is plotted on figures 1 through 8. The coring tool model without fins is unstable and showed a tendency to fall on its side under even the slightest angle of deviation (Figure 1). Increasing the separation distance for models with fins increased the righting moment (Figures 2, 3, 6). Rotating the vane orientation by 45° gave variable results (Figures 2, 4, 5). Fin 2 modified is superior to fin 1 from 0° to 16° (Figure 8). In general the reversed and reversed slotted types of fins proved to be superior in the range 0° to 12° to either fin 1 or fin 2 modified. A comparison of Appendix Tables A through V gives an indication of the range of superiority for each fin assembly.

Fin 6 reversed was the only fin that was superior to either fin 1 or fin 2 modified over the entire range of testing (Figure 8). A percentage comparison at the angles of 5°, 10°, and 15° shows fin 6 reversed to be 170 percent, 71 percent, and 32 percent respectively, superior to fin 1, and 25 percent, 20 percent and 16 percent respectively, superior to fin 2 modified. As previously noted an increase in the separation distance increases the righting moment. It is significant to note that the reversed fins could only be tested at a separation distance of 1.25 inches due to model design limitations, while fin 1 and fin 2 modified were tested at a separation distance of 2 inches. Therefore in actuality fin 6 reversed has a greater righting moment superiority than indicated.

Fin 4 reversed slotted was slightly inferior to fin 4 reversed for the range 0° to 11°. However above 11° its superiority is evident (Figure 5). This characteristic can be attributed to the fact that at higher angles the vanes are semi-exposed to the flow, instead of being shielded by the shroud, and therefore are capable of contributing to the righting

moment. Fin 6 could not be slotted because that fin had already been modified when the slotting phase of testing was done. However based on the results of fin 4 reversed slotted, fin 6 reversed slotted could test out to be the most desirable fin assembly.

For fins 3, 4, 5 and 6 the regular type created less drag than did the reversed type (Table 2). The drag coefficients which resulted because of the range of air speeds at which testing was conducted are nearly constants. (Figure 9).

Sediment types have different optimum penetration speeds which represent a compromise between sample disturbance and depth of penetration. In a fluid field, drag plus buoyant force equals the weight of the coring tool for non-accelerated cases. If the coefficient of drag for a particular coring tool - fin combination is known in addition to the optimum speed of descent, the weight necessary to attain that descent can be calculated. This presumes that the coring tool has the capability of having weight added, a presumption which is not valid for many of the present styles of coring tools.

Coring Tool Model (without fins)

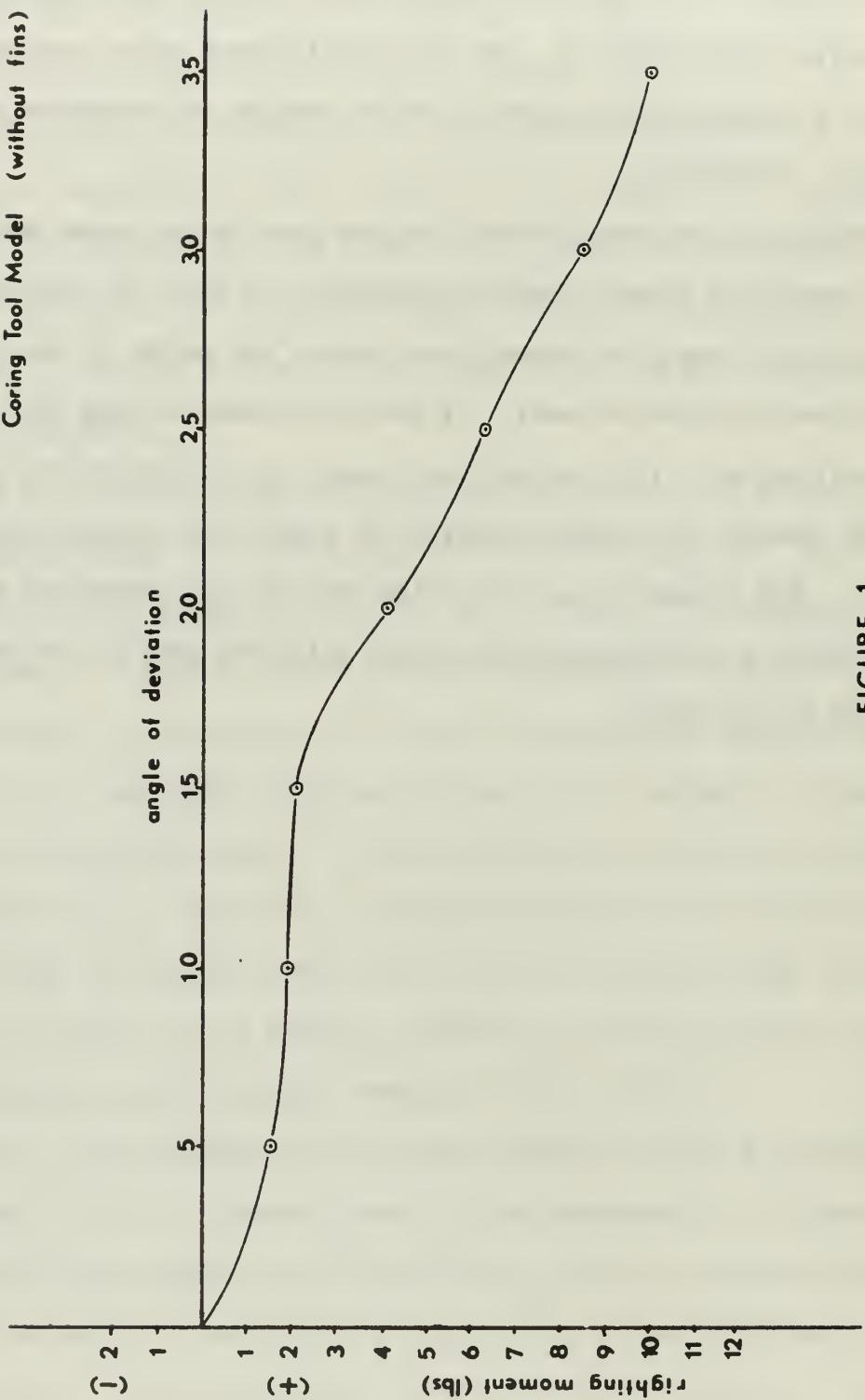


FIGURE 1

RIGHTING MOMENT "vs" ANGLE OF DEVIATION

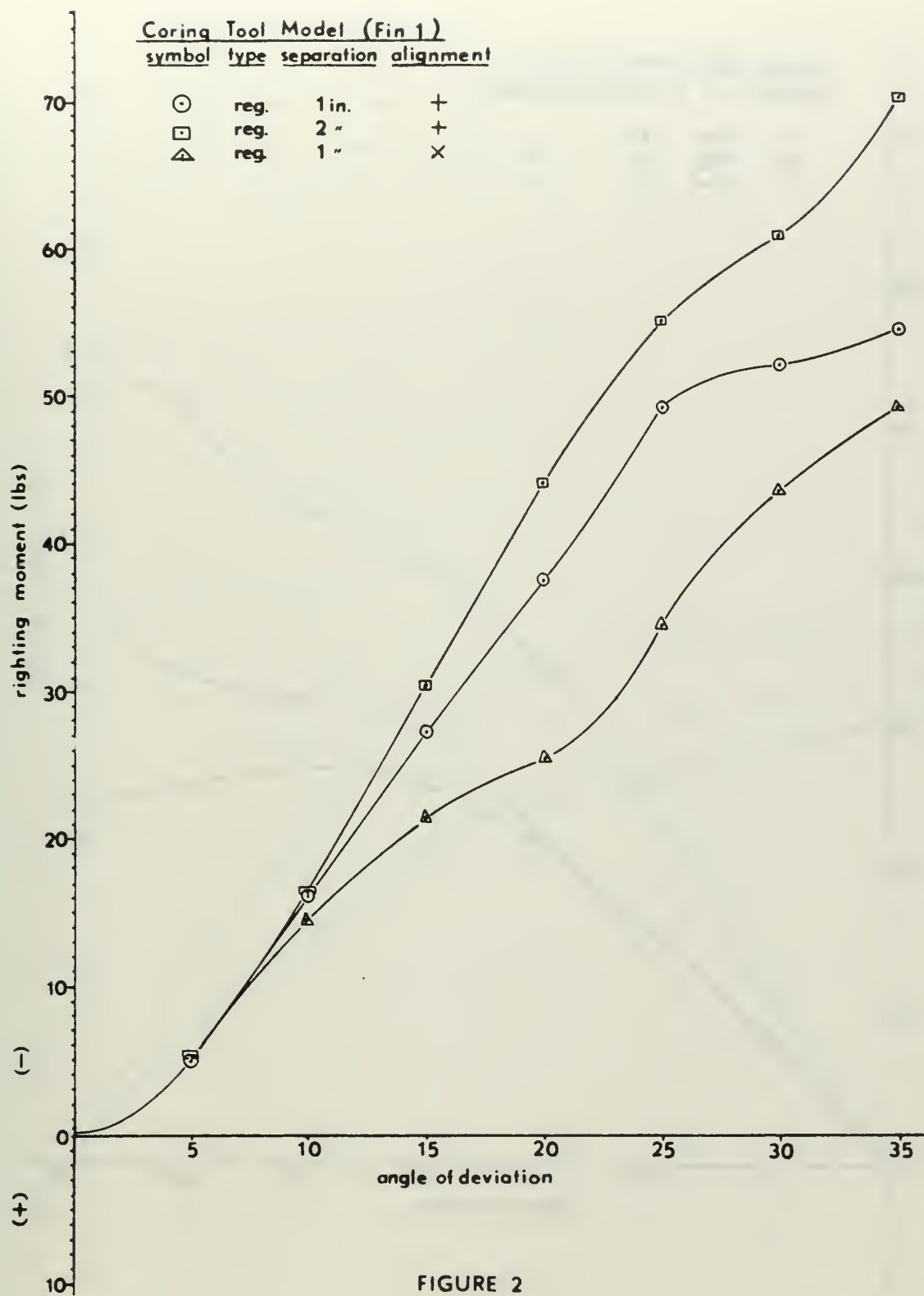


FIGURE 2

RIGHTING MOMENT "vs" ANGLE OF DEVIATION

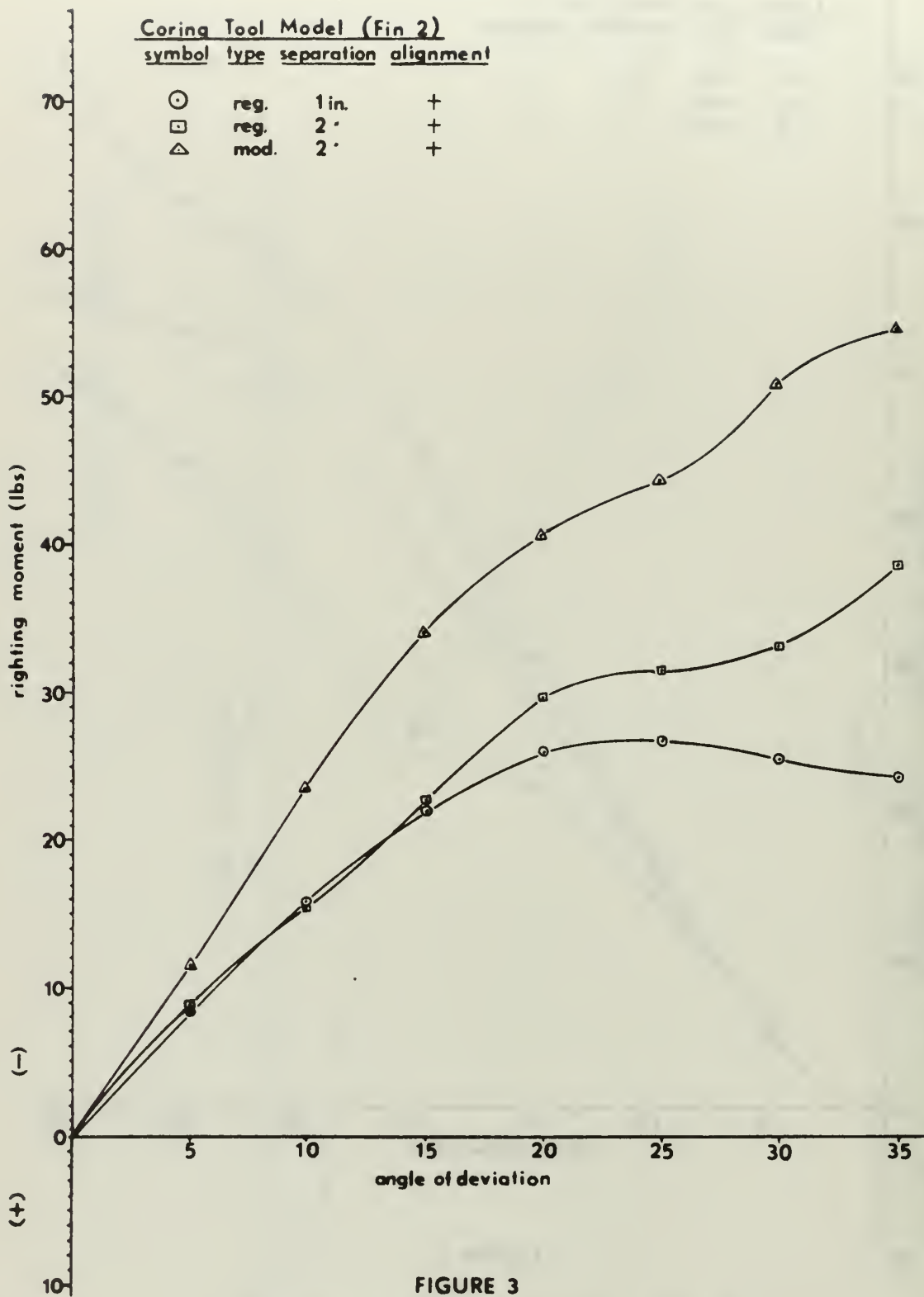


FIGURE 3

RIGHTING MOMENT "vs" ANGLE OF DEVIATION

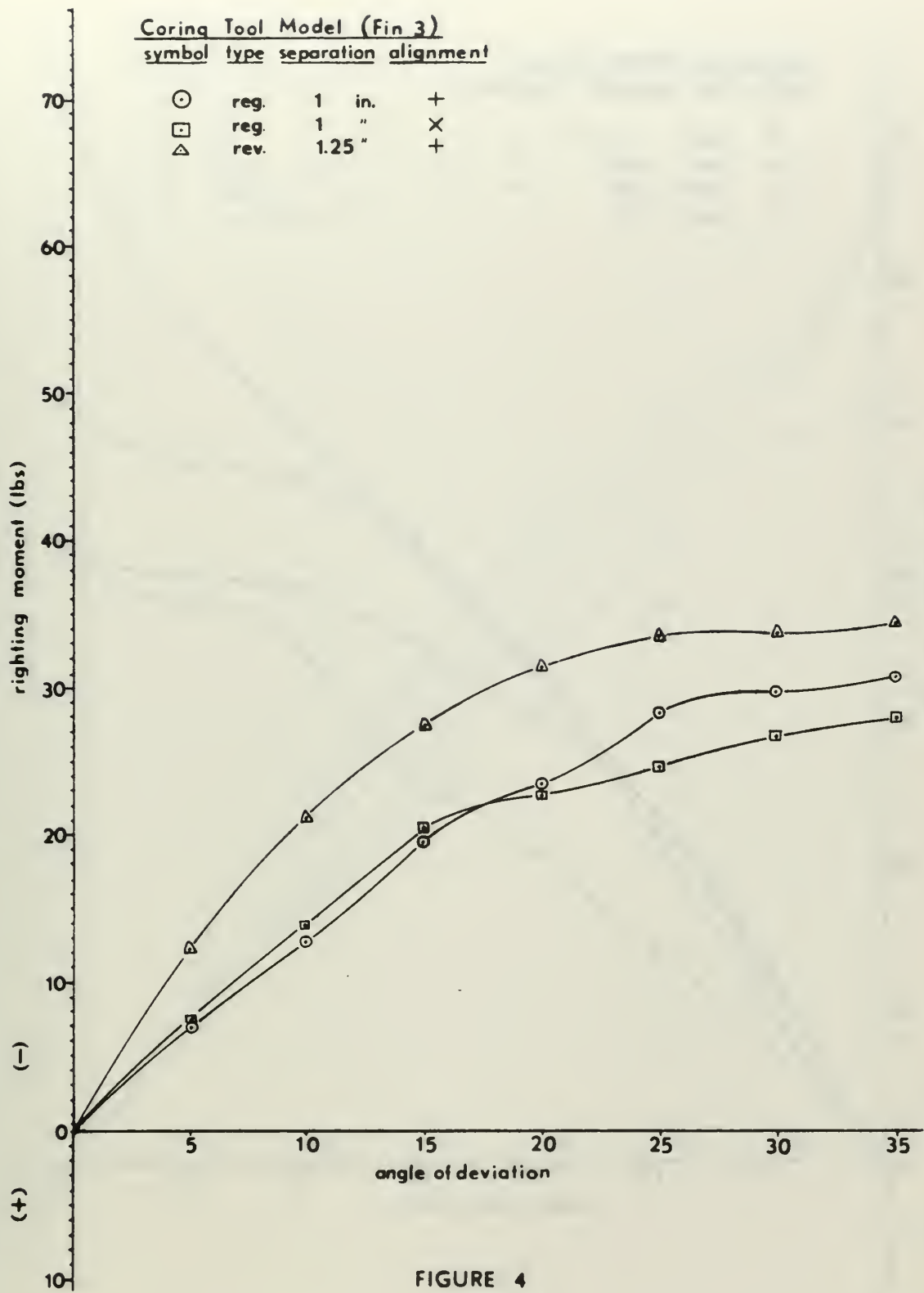


FIGURE 4

RIGHTING MOMENT "vs" ANGLE OF DEVIATION

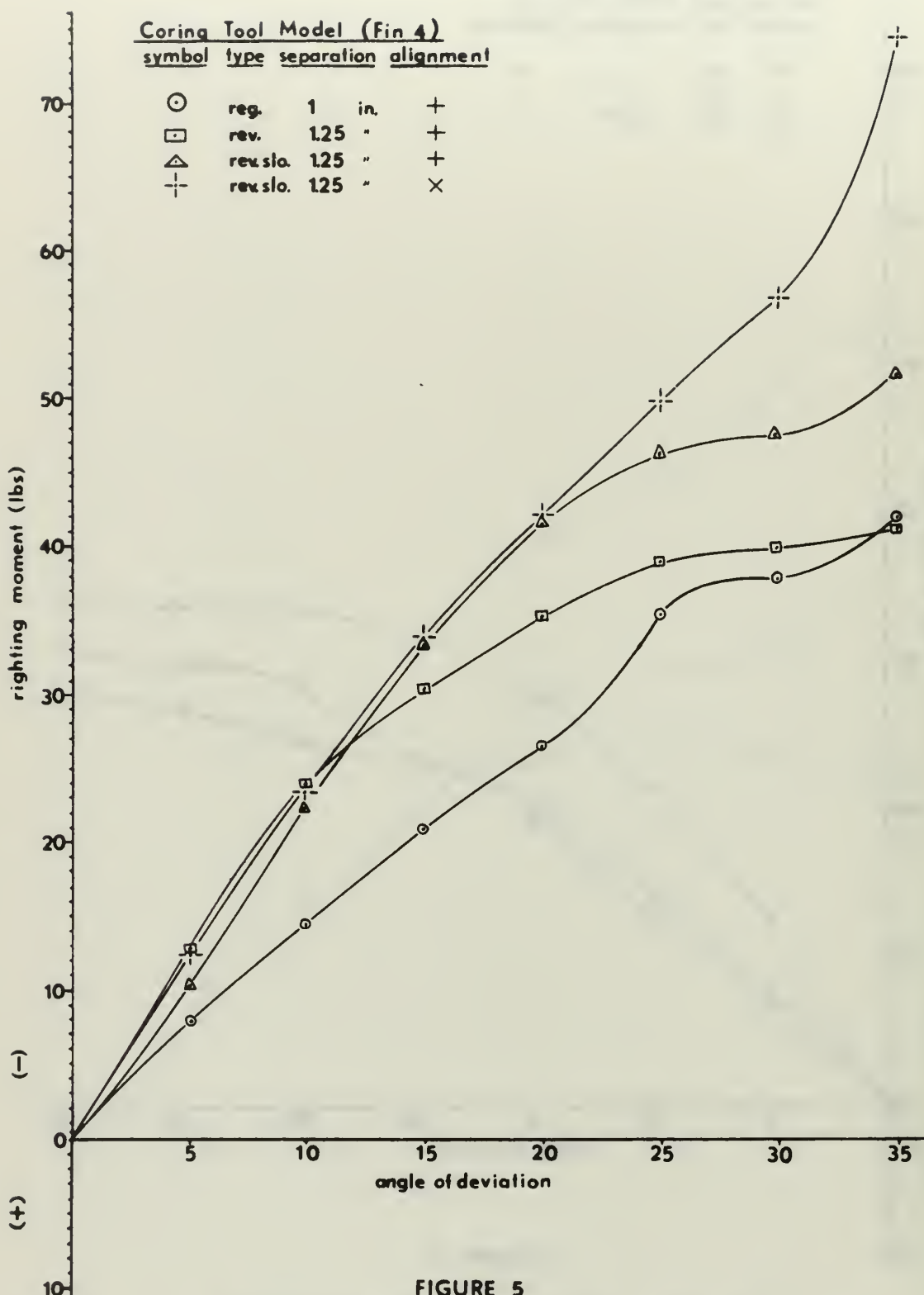


FIGURE 5

RIGHTING MOMENT "vs" ANGLE OF DEVIATION

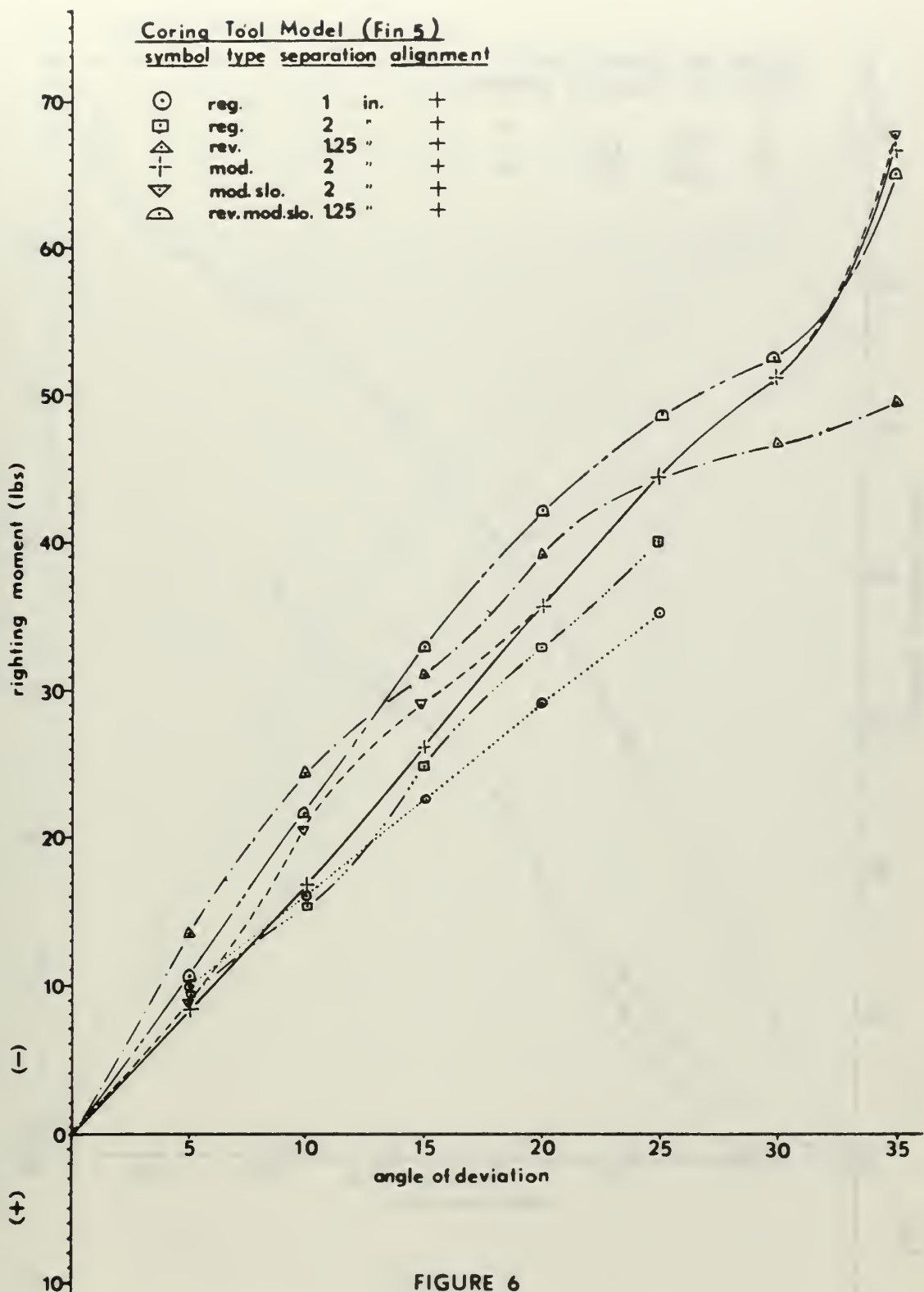


FIGURE 6

RIGHTING MOMENT "vs" ANGLE OF DEVIATION

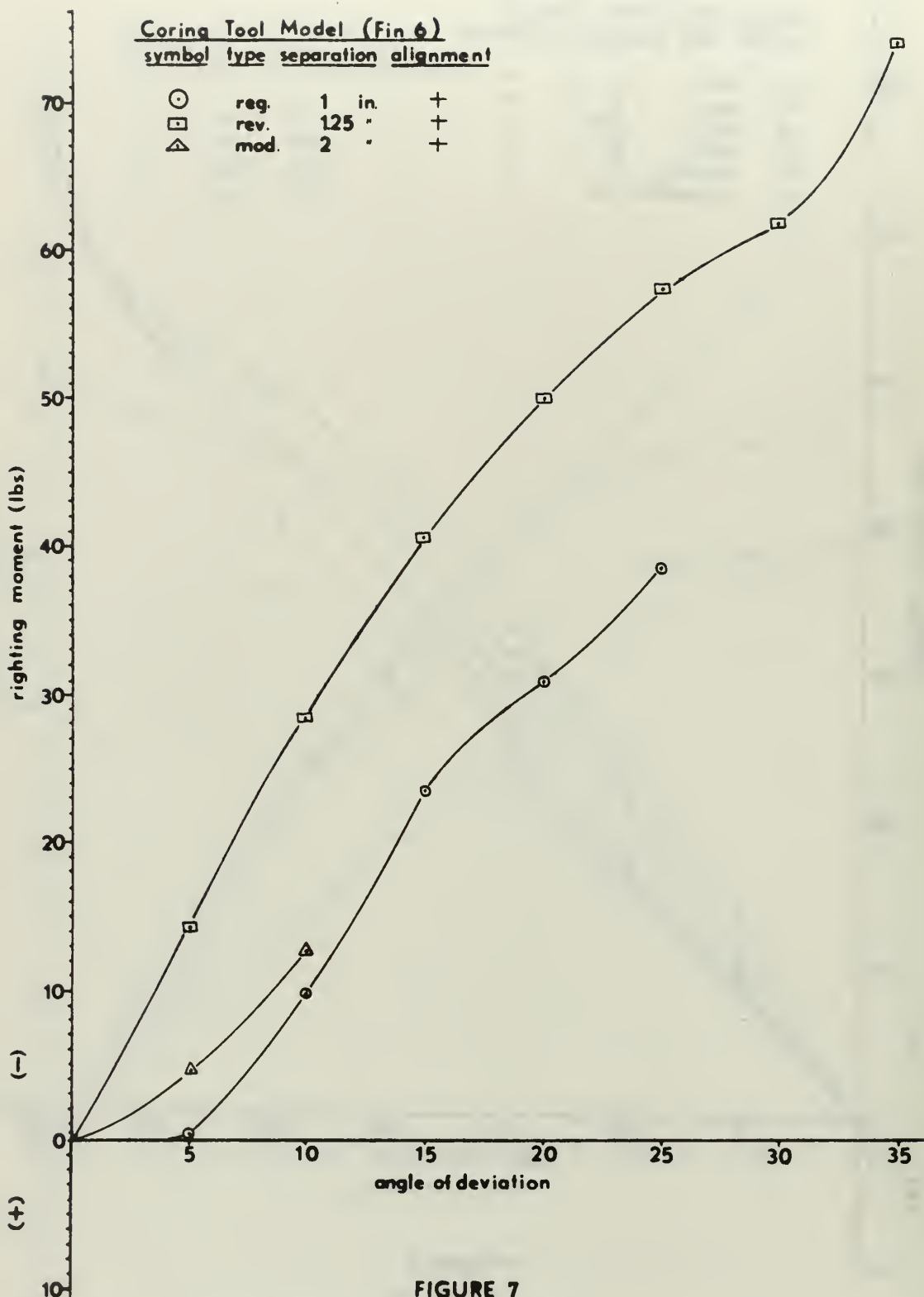


FIGURE 7

RIGHTING MOMENT "vs" ANGLE OF DEVIATION

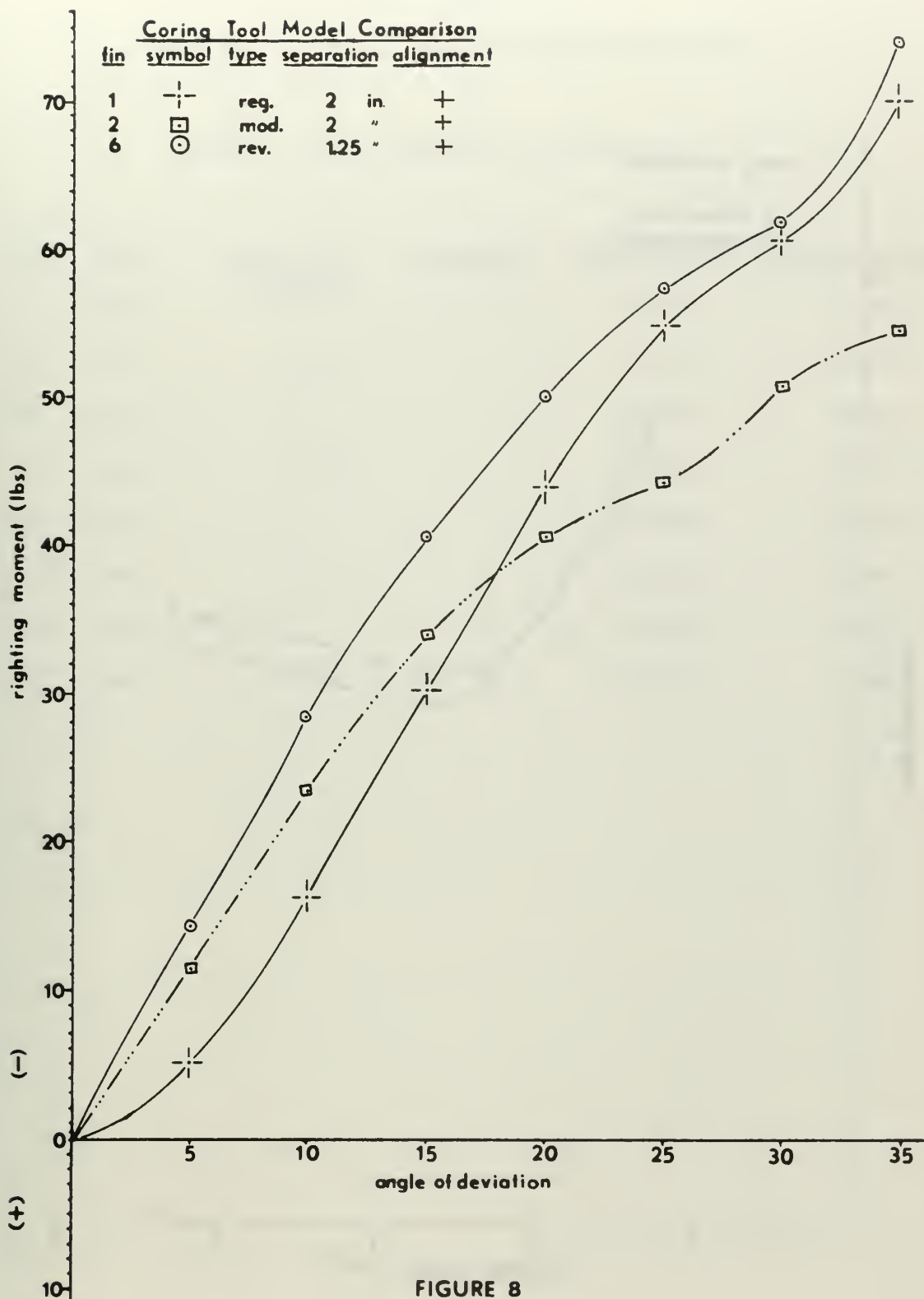


FIGURE 8

RIGHTING MOMENT "vs" ANGLE OF DEVIATION

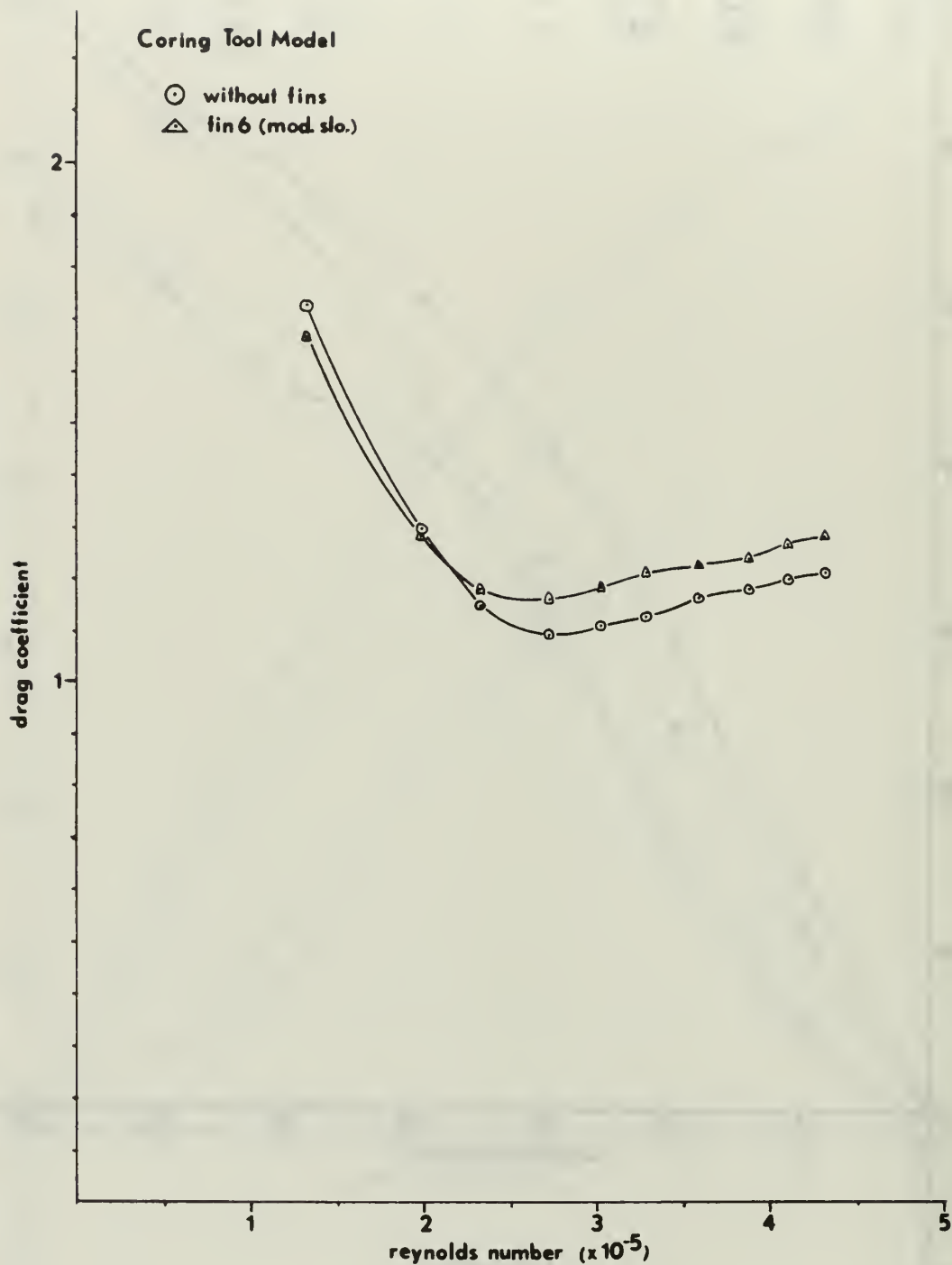


FIGURE 9

DRAG COEFFICIENT "vs" REYNOLDS NUMBER

TABLE 2  
 Comparison of Model Drag and Drag Coefficients  
 for  
 Fins 3, 4, 5, 6 (Regular and Reversed)

<u>Fin</u>	<u>Type</u>	<u>Separation (inches)</u>	<u>Alignment</u>	<u>Model Drag</u>	<u>Drag Coefficient</u>
3	reg.	1	+	+3.657	.728
3	rev.	1.25	+	+7.771	1.546
4	reg.	1	+	+4.324	.870
4	rev.	1.25	+	+8.923	1.836
5	reg.	2	+	+6.684	1.386
5	rev.	1.25	+	+9.886	2.069
6	reg.	1	+	+11.658	2.439
6	rev.	1.25	+	+12.171	2.506

#### SUMMARY COMMENTS

For coring tools whose shapes generally conform to the shape of the model used in this investigation, fin 6 reversed provides a superior righting moment. For a full scale coring tool the length of the fin assembly should be 94 percent of the longitudinal length of the driving weight. The apex of the cone from which the shroud is fabricated is 24°. The minimum exterior diameter of the shroud is 135 percent of the transverse dimension of the driving weight.

Based on test results it is evident that the stabilizing fin assembly should be placed as far above the driving weight as is possible. An optimum separation distance exists which varies with the length of the coring tool, the diameter of the coring tube, and the righting moment of the fin assembly. A cylindrical shaped body is prone to falling on its side regardless of its initial angle of entry into the fluid. It is necessary to measure, or calculate from theory, the + moment that the particular coring tube will exhibit through a range of angles. Knowing those moments, one can calculate the moment arm (separation distance) that the moment of the fin assembly must be multiplied by to cancel the + moment and insure a vertical descent.

A fin assembly designed for a particular shaped coring tool may prove to be the best assembly for that tool, but at the same time may prove to be an inferior assembly for another shaped tool. One reason for this is the type of fluid flow generated by the driving weight which effects the righting capability of the assembly. For example according to Streeter (1958) a tear shaped driving weight in subsonic flow creates much less turbulence and consequently drag, than the driving weight used on the model in this report. It is therefore suggested that driving weights be made tear shaped in addition to being adjustable.

It is possible to determine the moment and drag forces from theoretical calculations. However for complex bodies such as those studied in this report, wind tunnel testing has proven to be an accurate more rapid method.

It is evident from the general shape of the present type coring tools, fin shapes, and dearth of prior information that comparatively little study has been made in the area of coring tool stabilization.

REFERENCES

1. Hvorslev, M. J., 1949, Subsurface Exploration and Sampling of Soils for Civil Engineering Purposes. U. S. Army Corps of Engineers, Waterways Experiment Station, Vicksburg, Miss., p. 312.
2. Ohart, T. C., 1946, Elements of Ammunition, John Wiley & Sons, Inc., New York, pp. 207-208.
3. Pope, A., and J. J. Harper, 1966, Low-Speed Wind Tunnel Testing, John Wiley & Sons, Inc., New York, pp. 1-4.
4. Poston, E. R., 1948, Two-Component Characteristics of Thirty Bomb Fins Having a Common Leading Edge Attachment Point on the Afterbody, U. S. Navy Bureau of Ordnance Contract 9680, Univ. of Minnesota, Minneapolis, pp. 1-2.
5. Rosfelder, A. M., 1966, Subsea Coring for Geological and Geotechnical Surveys, Univ. of California, San Diego, p. 713.
6. Schlichting, H., 1960, Boundary Layer Theory, Trans. J. Kestin, McGraw-Hill Book Company, Inc., New York, pp. 8-9.
7. Streeter, V. L., 1958, Fluid Mechanics, McGraw-Hill Book Company, Inc., New York, pp. 138, 171, 174, 230.

## APPENDIX

### Symbols and Nomenclature for Tables A-W

$\alpha_{bal}$  ..... angle in degrees indicated by the beam balance pitch indicator

$\alpha$  ..... angle of deviation of the model in angular degrees

Alignment .... refers to vane orientation with respect to horizontal

$C_D$  ..... coefficient of drag

$C_m (H_2O)$  ..... centimeter height of the micromanometer

#### Drag

gross..... registered in pounds by the beam balance

support.... drag created by the struts

model..... gross drag minus support drag

fin..... that portion of the model drag created by the fin assemblies attached to the model

#### Moment

gross..... registered in pounds by the beam balance

tare..... a static moment that exists because of the distribution of the weight of the model on the struts with no wind force being applied

net..... gross drag minus tare drag

adjusted... obtained by subtracting the net moment at zero degrees from each of the net moments 0 to 35 degrees

$R_e$  ..... Reynolds number

Separation.... minimum distance from the rear of the driving weight to the most forward part of the fin assembly

Speed..... refers to wind tunnel air speed

#### Type

regular.... (reg.), tapered edge (leading edge) of vanes are pointed toward the driving weight

reversed... (rev.), tapered edge of vanes are pointed away from the driving weight

modified... (mod.), exterior shroud is cut back to the point of intersection of vane and shroud

slotted.... (slo.), longitudinal strips are cut from the shroud on either side of the vanes

TABLE A

CORING TOOL MODEL (Fin 1)

Type: Regular

Separation: 1 inch

Alignment: +

$\alpha_{bal.}$	$\alpha$	gross moment in lbs.	tare moment in lbs.	net moment in lbs.	adjusted moment in lbs.	temp. °F	cm. H <sub>2</sub> O	speed m.p.h.
29'	0	-3.15	-	-3.15	0	83.5	50.62	201.06
5°25'	5	-8.59	-.50	-8.09	-4.94	-	-	-
10°25'	10	-20.13	-.88	-19.25	-16.10	96	49.32	198.46
15°30'	15	-32.10	-1.64	-30.46	-27.31	99	48.17	196.13
20°30'	20	-43.18	-2.52	-40.66	-37.51	102	48.13	196.05
25°30'	25	-56.32	-3.83	-52.49	-49.34	102	47.65	195.07
30°25'	30	-60.41	-5.18	-55.23	-52.08	104	46.92	193.57
35°25'	35	-64.40	-6.69	-57.71	-54.56	105	46.35	192.39

$\alpha$	gross drag lbs.	support drag lbs.	model drag lbs.	fin drag lbs.	$C_D$
0	+5.522	+2.598	+2.924	.031	.586
5	+5.779				
10	+6.428				
15	+7.540				
20	+9.378				
25	+11.094				
30	+12.90				
35	+14.45				

TABLE B

## CORING TOOL MODEL (Fin 1)

Type: Regular

Separation: 1 inch

Alignment: X

$\alpha_{bal.}$	$\infty$	gross moment in lbs.	tare moment in lbs.	net moment in lbs.	adjusted moment in lbs.	temp. °F	cm. $H_2O$	speed m.p.h.
29°	0	- 3.69	-	- 3.69	0	96	49.31	198.44
5°25'	5	- 9.26	- .50	- 8.76	- 5.07	102	48.48	196.76
10°25'	10	-16.40	- .88	-15.52	-14.64	104	48.49	196.76
15°30'	15	-24.89	-1.64	-23.25	-21.61	104	48.49	196.76
20°30'	20	-31.90	-2.52	-29.38	-25.69	105	47.98	195.75
25°30'	25	-42.41	-3.83	-38.58	-34.89	106	47.54	194.85
30°25'	30	-52.60	-5.18	-47.42	-43.73	-	-	-
35°25'	35	-59.81	-6.69	-53.12	-49.43	-	-	-

$\infty$	gross drag lbs.	support drag lbs.	model drag lbs.	fin drag lbs.	$C_D$
0	+ 5.393	+2.598	+2.795	- .098	.573
5	+ 5.664				
10	+ 6.157				
15	+ 7.092				
20	+ 8.940				
25	+ 9.920				
30	+11.917				
35	+14.800				

TABLE C

## CORING TOOL MODEL (Fin 1)

Type: Regular

Separation: 2"

Alignment: +

$\alpha_{bal.}$	$\alpha$	gross moment in lbs.	tare moment in lbs.	net moment in lbs.	adjusted moment in lbs.	temp. °F	cm. H <sub>2</sub> O	speed m.p.h.
+ 30'	0	- 2.64	-	- 2.64	0	92	49.66	199.14
+ 5°40'	5	- 8.04	- .29	- 7.75	- 5.11	-	-	-
+10°55'	10	-19.59	- .54	-19.05	-16.41	97	48.68	197.17
+16°15'	15	-34.48	-1.26	-33.22	-30.58	-	-	-
+21°30'	20	-48.99	-2.24	-46.75	-44.11	100	47.86	195.50
+26°45'	25	-61.26	-3.39	-57.87	-55.23	-	-	-
+32°10'	30	-68.44	-4.86	-63.58	-60.94	102	46.66	193.03
+37°30'	35	-79.51	-6.50	-73.01	-70.37	-	-	-

$\alpha$	gross drag lbs.	support drag lbs.	model drag lbs.	fin drag lbs.	$C_D$
0	+ 6.190	+2.598	+3.592	+ .699	.733
5	+ 6.120				
10	+ 6.656				
15	+ 7.854				
20	+ 9.675				
25	+11.690				
30	+13.750				
35	+15.340				

TABLE D

CORING TOOL MODEL (Fin 2)

Type: Regular

Separation: 1 inch

Alignment: +

$\alpha_{bal.}$	$\alpha$	gross moment in lbs.	tare moment in lbs.	net moment in lbs.	adjusted moment in lbs.	temp. °F	cm. $H_2O$	speed m.p.h.
+ 15'	0	- 2.66	-	- 2.66	0	62	53.48	206.66
+ 5°10'	5	-11.36	- .32	-11.04	- 8.38	-	-	-
+10°10'	10	-19.22	- .63	-18.59	-15.93	-	-	-
+15°10'	15	-25.93	-1.32	-24.61	-21.95	81	49.60	199.02
+20°10'	20	-30.84	-2.25	-28.59	-25.93	-	-	-
+25°15'	25	-32.59	-3.47	-29.12	-26.46	86	48.92	197.65
+30°10'	30	-32.57	-4.79	-27.78	-25.12	-	-	-
+35°10'	35	-33.01	-6.56	-26.45	-23.79	90	47.92	195.62

$\alpha$	gross drag lbs.	support drag lbs.	model drag lbs.	fin drag lbs.	$C_D$
0	+ 8.557	+2.598	+5.959	+3.066	1.130
5	+ 8.566				
10	+ 8.880				
15	+ 9.648				
20	+10.885				
25	+12.231				
30	+13.471				
35	+14.586				

TABLE E

## CORING TOOL MODEL (Fin 2)

Type: Regular

Separation: 2 inch

Alignment: +

$\alpha_{bal.}$	$\alpha C$	gross moment in lbs.	tare moment in lbs.	net moment in lbs.	adjusted moment in lbs.	temp. °F	cm. $H_2O$	speed m.p.h.
+ 30'	0	- 3.44	-	- 3.44	0	91	49.47	198.76
+ 5°40'	5	-12.21	- .13	-12.08	- 8.64	-	-	-
+10°55'	10	-19.56	- .65	-18.91	-15.47	97	48.73	197.27
+16°15'	15	-27.19	-1.32	-25.87	-22.43	-	-	-
+21°30'	20	-35.40	-2.50	-32.90	-29.46	100	48.03	195.85
+26°45'	25	-38.82	-3.95	-34.87	-31.43	-	-	-
+32°10'	30	-42.00	-5.62	-36.38	-32.94	101	46.76	193.24
+37°30'	35	-49.24	-7.49	-41.75	-38.31	-	-	-

$\alpha C$	gross drag lbs.	support drag lbs.	model drag lbs.	fin drag lbs.	$C_D$
0	+ 7.319	+2.598	+4.721	+1.828	.968
5	+ 7.350				
10	+ 7.815				
15	+ 8.632				
20	+10.227				
25	+11.284				
30	+12.350				
35	+14.068				

TABLE F

## CORING TOOL MODEL (Fin 2)

Type: Modified

Separation: 2 inch

Alignment: +

$\alpha_{bal.}$	$\infty$	gross moment in lbs.	tare moment in lbs.	net moment in lbs.	adjusted moment in lbs.	temp. °F	cm. $H_2O$	speed m.p.h.
+ 30°	0	- 3.57	-	- 3.57	0	74	51.48	202.76
+ 5°40'	5	-15.35	- .29	-15.06	-11.49	-	-	-
+10°55'	10	-27.39	- .42	-26.97	-23.40	83	50.03	199.88
+16°15'	15	-38.92	-1.31	-37.61	-34.04	-	-	-
+21°30'	20	-46.73	-2.44	-44.37	-40.80	87	48.72	197.25
+26°45'	25	-51.80	-3.76	-48.04	-44.47	-	-	-
+32°10'	30	-59.73	-5.41	-54.32	-50.75	90	47.88	195.54
+37°30'	35	-65.09	-7.23	-57.86	-54.29	93	-	-

$\infty$	gross drag lbs.	support drag lbs.	model drag lbs.	fin drag lbs.	$C_D$
0	+ 7.058	+2.598	+4.460	+1.567	.879
5	+ 7.091				
10	+ 7.634				
15	+ 8.670				
20	+10.141				
25	+11.311				
30	+13.567				
35	+15.254				

TABLE G

## CORING TOOL MODEL (Fin 3)

Type: Regular

Separation: 1 inch

Alignment: +

$\alpha_{bal.}$	$\infty$	gross moment in lbs.	tare moment in lbs.	net moment in lbs.	adjusted moment in lbs.	temp. °F	cm. $H_2O$	speed m.p.h.
+ 15'	0	- 3.20	-	- 3.20	0	87	50.93	201.67
+ 5°10'	5	-10.38	- .23	-10.15	- 6.95	-	-	-
+10°10'	10	-16.54	- .60	-15.94	-12.74	95	49.74	199.30
+15°10'	15	-23.77	-1.13	-22.64	-19.44	-	-	-
+20°10'	20	-28.84	-2.25	-26.59	-23.39	98	48.78	197.37
+25°15'	25	-34.72	-3.49	-31.23	-28.03	-	-	-
+30°10'	30	-37.90	-4.91	-32.99	-29.79	100	47.92	195.62
35°10'	35	-40.48	-6.62	-33.86	-30.66	100	-	-

$\infty$	gross drag lbs.	support drag lbs.	model drag lbs.	fin drag lbs.	$C_D$
0	+ 6.255	+2.598	+3.657	+ .764	.728
5	+ 6.50				
10	+ 7.120				
15	+ 8.229				
20	+ 9.677				
25	+11.582				
30	+13.483				
35	+15.280				

TABLE H  
CORING TOOL MODEL (Fin 3)

Type: Regular

Separation: 1 inch

Alignment: X

$\alpha_{bal.}$	$\alpha$	gross moment in lbs.	face moment in lbs.	net moment in lbs.	adjusted moment in lbs.	temp. °F	cm. $H_2O$	speed m.p.h.
+ 15°	0	- 3.48	-	- 3.48	0	99	49.57	198.96
+ 5°10'	5	-10.74	- .23	-10.51	- 7.03	-	-	-
+10°10'	10	-18.00	- .60	-17.40	-13.92	102	48.86	197.53
+15°10'	15	-24.90	-1.13	-23.77	-20.29	-	-	-
+20°10'	20	-28.41	-2.25	-26.16	-22.68	104	48.32	196.44
+25°15'	25	-31.61	-3.49	-28.12	-24.64	-	-	-
+30°10'	30	-34.79	-4.91	-29.88	-26.40	106	47.03	193.80
+35°10'	35	-37.71	-6.62	-31.09	-27.61	-	-	-

$\alpha$	gross drag lbs.	support drag lbs.	model drag lbs.	fin drag lbs.	$C_D$
0	+ 6.091	+2.598	+3.493	+ .600	.714
5	+ 6.367				
10	+ 7.086				
15	+ 8.157				
20	+ 9.640				
25	+11.177				
30	+12.848				
35	+14.538				

TABLE I  
CORING TOOL MODEL (Fin 3)

Type: Reversed

Separation: 1.25 inch

Alignment: +

$\alpha_{bal.}$	$\infty$	gross moment in lbs.	tare moment in lbs.	net moment in lbs.	adjusted moment in lbs.	temp. °F	cm. $H_2O$	speed m.p.h.
+ 30'	0	- 3.90	-	- 3.90	0	72	50.97	201.75
+ 5°40'	5	-16.19	- .09	-16.10	-12.20	-	-	-
+10°55'	10	-25.31	- .28	-25.03	-21.13	81	49.92	199.66
+16°15'	15	-32.56	-1.35	-31.21	-27.31	-	-	-
+21°30'	20	-37.68	-2.34	-35.34	-31.44	85	49.13	198.08
+26°45'	25	-41.13	-3.79	-37.34	-33.44	-	-	-
+32°10'	30	-42.92	-5.48	-37.44	-33.54	88	47.97	195.72
+37°30'	35	-45.49	-7.43	-38.06	-34.16	90	-	-

$\infty$	gross drag lbs.	support drag lbs.	model drag lbs.	fin drag lbs.	$C_D$
0	+10.369	+2.598	+7.771	+4.878	1.546
5	+10.231				
10	+10.463				
15	+11.145				
20	+12.274				
25	+13.474				
30	+14.691				
35	+16.03				

TABLE J

CORING TOOL MODEL (Fin 4)

Type: Regular

Separation: 1 inch

Alignment: +

$\alpha_{bal.}$	$\alpha$	gross moment in lbs.	tare moment in lbs.	net moment in lbs.	adjusted moment in lbs.	temp. °F	cm. H <sub>2</sub> O	speed m.p.h.
+ 15°	0	- 3.32	-	- 3.32	0	89	50.40	200.62
+ 5°10'	5	-11.150	- .21	-10.94	- 7.62	-	-	-
+10°10'	10	-18.21	- .50	-17.71	-14.39	95	49.44	198.70
+15°10'	15	-25.23	-1.23	-24.00	-20.68	-	-	-
+20°10'	20	-31.69	-2.23	-29.46	-26.14	98	48.42	196.64
+25°15'	25	-38.84	-3.46	-38.38	-35.06	-	-	-
+30°10'	30	-45.98	-4.89	-41.09	-37.77	101	47.47	194.70
+35°10'	35	-51.69	-6.64	-45.05	-41.73	103	-	-

$\alpha$	gross drag lbs.	support drag lbs.	model drag lbs.	fin drag lbs.	$C_D$
0	+ 6.922	+2.598	+4.324	+1.431	.870
5	+ 7.207				
10	+ 7.847				
15	+ 8.832				
20	+10.248				
25	+12.218				
30	+14.508				
35	+16.422				

TABLE K

## CORING TOOL MODEL (Fin 4)

Type: Reversed

Separation: 1.25 inch

Alignment: +

$\alpha_{bal.}$	$\alpha$	gross moment in lbs.	tare moment in lbs.	net moment in lbs.	adjusted moment in lbs.	temp. °F	cm. H <sub>2</sub> O	speed m.p.h.
+ 30°	0	- 3.51	-	- 3.51	0	89	49.31	198.44
+ 5°40'	5	-16.48	- .07	-16.41	-12.90	-	-	-
+10°55'	10	-28.03	- .55	-27.48	-23.97	96	48.32	196.44
+16°15'	15	-35.17	-1.34	-33.83	-30.32	-	-	-
+21°30'	20	-40.99	-2.45	-38.54	-35.03	-	-	-
+26°45'	25	-46.08	-3.80	-42.28	-38.77	101	47.17	194.09
+32°10'	30	-48.82	-5.56	-43.26	-39.75	-	-	-
+37°30'	35	-52.07	-7.57	-44.50	-40.99	103	46.24	192.16

$\alpha$	gross drag lbs.	support drag lbs.	model drag lbs.	fin drag lbs.	$C_D$
0	+11.521	+2.598	+8.923	+6.030	1.836
5	+11.293				
10	+11.564				
15	+11.90				
20	+12.839				
25	+13.845				
30	+14.971				
35	+16.061				

TABLE I

## CORING TOOL MODEL (Fin 4)

Type: Reversed, slotted

Separation: 1.25 inch

Alignment: +

$\alpha_{bal.}$	$\infty$	gross moment in lbs.	tare moment in lbs.	net moment in lbs.	adjusted moment in lbs.	temp. °F	cm. H <sub>2</sub> O	speed m.p.h.
+ 30'	0	- 3.48	-	- 3.48	0	60	54.05	207.76
+ 5°40'	5	-13.77	- .19	-13.58	-10.10	-	-	-
+10°55'	10	-26.33	- .52	-25.81	-22.33	68	52.56	204.88
+16°15'	15	-37.78	-1.10	-36.68	-33.20	-	-	-
+21°30'	20	-46.84	-2.23	-44.61	-41.43	75	51.10	202.01
+26°45'	25	-53.25	-3.53	-49.72	-46.24	-	-	-
+32°10'	30	-56.22	-5.23	-50.99	-47.51	80	49.27	198.36
+37°30'	35	-61.92	-6.93	-54.99	-51.51	83	47.85	195.48

$\infty$	gross drag lbs.	support drag lbs.	model drag lbs.	fin drag lbs.	$C_D$
0	+ 7.816	+2.598	+5.218	+2.325	.979
5	+ 7.867				
10	+ 8.560				
15	+ 8.721				
20	+11.066				
25	+12.587				
30	+14.212				
35	+16.151				

TABLE M

## CORING TOOL MODEL (Fin 4)

Type: Reversed, slotted

Separation: 1.25 inch

Alignment: X

$\alpha_{bal.}$	$\alpha$	gross moment in lbs.	tare moment in lbs.	net moment in lbs.	adjusted moment in lbs.	temp. °F	cm. $H_2O$	speed m.p.h.
+ 30°	0	- 1.43	-	- 1.43	0	74	52.14	204.05
+ 5°40'	5	-13.95	- .19	-13.76	-12.33	-	-	-
+10°55'	10	-25.01	- .52	-24.49	-23.06	81	50.90	201.61
+16°15'	15	-36.22	-1.10	-35.12	-33.69	-	-	-
+21°30'	20	-45.47	-2.23	-43.24	-41.81	85	49.90	199.62
+26°45'	25	-54.68	-3.53	-51.15	-49.72	-	-	-
+32°10'	30	-63.53	-5.23	-58.30	-56.87	88	48.82	197.45
37°30'	35	-82.71	-6.93	-75.78	-74.35	92	47.03	193.80

$\alpha$	gross drag lbs.	support drag lbs.	model drag lbs.	fin drag lbs.	$C_D$
0	+ 7.508	+2.598	+4.910	+2.017	.955
5	+ 7.670				
10	+ 8.350				
15	+ 9.444				
20	+10.981				
25	+12.667				
30	+14.669				
35	+16.889				

TABLE N

## CORING TOOL MODEL (Fin 5)

Type: Regular

Separation: 1 inch

Alignment: +

$\alpha_{bal.}$	$\alpha_C$	gross moment in lbs.	tare moment in lbs.	net moment in lbs.	adjusted moment in lbs.	temp. °F	cm. $H_2O$	speed m.p.h.
+ 15°	0	- 3.37	-	- 3.37	0	95	49.44	198.70
+ 5°10'	5	-13.90	- .18	-13.72	-10.35	-	-	-
+10°10'	10	-20.10	- .55	-19.55	-16.18	98	48.67	197.15
+15°10'	15	-27.47	-1.33	-26.14	-22.77	-	-	-
+20°10'	20	-34.94	-2.38	-32.56	-29.19	101	48.18	196.15
+25°15'	25	-42.50	-3.79	-38.71	-35.34	103	47.05	193.84
+30°10'	30	-	-	-	-	-	-	-
+35°10'	35	-	-	-	-	-	-	-

$\alpha_C$	gross drag lbs.	support drag lbs.	model drag lbs.	fin drag lbs.	$C_D$
0	+ 9.282	+2.598	+6.684	+3.791	1.371
5	+ 9.395				
10	+ 9.753				
15	+10.566				
20	+11.923				
25	+13.582				
30					
35					

TABLE 0

CORING TOOL MODEL (Fin 5)

Type: Regular

Separation: 2 inch

Alignment: +

$\alpha_{bal.}$	$\alpha$	gross moment in lbs.	tare moment in lbs.	net moment in lbs.	adjusted moment in lbs.	temp. °F	cm. H <sub>2</sub> O	speed m.p.h.
+ 30°	0	- 3.44	-	- 3.44	0	95	48.90	197.61
+ 5°40'	5	-13.33	- .20	-13.13	- 9.69	-	-	-
+10°55'	10	-19.61	- .61	-19.00	-15.56	99	48.19	196.17
+16°15'	15	-30.18	-1.60	-28.58	-25.14	-	-	-
+21°30'	20	-39.24	-2.75	-36.49	-33.05	101	47.05	193.84
+26°45'	25	-48.00	-4.19	-43.81	-40.37	103	-	-
+32°10'	30	-	-	-	-	-	-	-
+37°30'	35	-	-	-	-	-	-	-

Note: Test was aborted at  $\alpha$  = 25 degrees due to excessive vibrations

$\alpha$	gross drag lbs.	support drag lbs.	model drag lbs.	fin drag lbs.	$C_D$
0	+ 9.382	+2.598	+6.684	+3.791	1.386
5	+ 9.428				
10	+ 9.750				
15	+10.750				
20	+12.195				
25	+13.666				
30	-				
35	-				

TABLE P

## CORING TOOL MODEL (Fin 5)

Type: Reversed

Separation: 1.25 inch

Alignment: +

$\alpha_{bal.}$	$\alpha$	gross moment in lbs.	tare moment in lbs.	net moment in lbs.	adjusted moment in lbs.	temp. °F	cm. H <sub>2</sub> O	speed m.p.h.
+ 30°	0	- 3.23	-	- 3.23	0	96	48.49	196.78
+ 5°40'	5	-16.92	- .13	-16.79	-13.56	-	-	-
+10°55'	10	-28.32	- .69	-27.63	-24.40	-	-	-
+16°15'	15	-36.00	-1.75	-34.25	-31.02	101	47.49	194.74
+21°30'	20	-45.06	-2.55	-42.51	-39.28	-	-	-
+26°45'	25	-51.84	-4.04	-47.80	-44.57	103	46.50	192.70
+32°10'	30	-55.80	-5.78	-50.02	-46.79	-	-	-
+37°30'	35	-60.49	-7.79	-52.70	-49.47	105	45.53	190.68

$\alpha$	gross drag lbs.	support drag lbs.	model drag lbs.	fin drag lbs.	$C_D$
0	+12.484	+2.598	+9.886	+6.993	2.069
5	+12.546				
10	+12.525				
15	+12.708				
20	+13.774				
25	+14.780				
30	+15.780				
35	+17.092				

TABLE Q

CORING TOOL MODEL (Fin 5)

Type: Modified

Separation: 2 inch

Alignment: +

$\infty_{bal.}$	$\infty$	gross moment in lbs.	tare moment in lbs.	net moment in lbs.	adjusted moment in lbs.	temp. °F	cm. $H_2O$	speed m.p.h.
+ 30'	0	- 3.26	-	- 3.26	0	87	49.48	198.78
+ 5°40'	5	-12.00	- .30	-11.70	- 8.44	-	-	-
+10°55'	10	-20.85	- .64	-20.21	-16.95	93	48.59	196.99
+16°15'	15	-30.74	-1.46	-29.28	-26.02	-	-	-
+21°30'	20	-41.69	-2.56	-39.13	-35.87	96	47.98	195.75
+26°45'	25	-51.44	-3.92	-47.52	-44.26	-	-	-
+32°10'	30	-60.00	-5.67	-54.33	-51.07	98	46.94	193.61
+37°30'	35	-77.28	-7.60	-69.68	-66.42	100	-	-

$\infty$	gross drag lbs.	support drag lbs.	model drag lbs.	fin drag lbs.	$C_D$
0	+ 7.682	+2.598	+5.084	+2.191	1.042
5	+ 7.831				
10	+ 8.426				
15	+ 9.465				
20	+11.181				
25	+12.790				
30	+14.652				
35	+16.467				

TABLE R

## CORING TOOL MODEL (Fin 5)

Type: Modified slotted

Separation: 2 inch

Alignment: +

$\alpha_{bal.}$	$\infty$	gross moment in lbs.	tare moment in lbs.	net moment in lbs.	adjusted moment in lbs.	temp. °F	cm. $H_2O$	speed m.p.h.
+ 30°	0	- 4.01	-	- 4.01	0	72	52.84	205.42
+ 5°40'	5	-12.89	- .16	-12.73	- 8.72	-	-	-
+10°55'	10	-25.25	- .55	-24.70	-20.69	81	51.37	202.54
+16°15'	15	-34.18	-1.22	-32.96	-28.95	-	-	-
+21°30'	20	-41.70	-2.24	-39.46	-35.45	85	50.10	200.02
+26°45'	25	-51.92	-3.54	-48.38	-44.37	-	-	-
+32°10'	30	-60.36	-5.15	-55.21	-51.20	89	48.96	197.73
+37°30'	35	-78.29	-6.75	-71.54	-67.53	93	47.03	193.80

$\infty$	gross drag lbs.	support drag lbs.	model drag lbs.	fin drag lbs.	$C_D$
0	+ 6.709	+2.598	+4.111	+1.218	.789
5	+ 6.811				
10	+ 7.561				
15	+ 8.753				
20	+10.346				
25	+12.164				
30	+14.117				
35	+16.025				

TABLE S

CORING TOOL MODEL (Fin 5)

Type: Modified Slotted Reversed

Separation: 1.25 inch

Alignment: +

$\alpha_{bal.}$	$\alpha$	gross moment in lbs.	tare moment in lbs.	net moment in lbs.	adjusted moment in lbs.	temp. °F	cm. H <sub>2</sub> O	speed m.p.h.
+ 30°	0	- 4.19	-	- 4.19	0	82	51.26	202.33
+ 5°40'	5	-14.64	- .18	-14.46	-10.27	-	-	-
+10°55'	10	-26.68	- .58	-26.10	-21.91	89	50.28	200.38
+16°15'	15	-38.53	-1.29	-37.24	-33.05	-	-	-
+21°30'	20	-48.74	-2.19	-46.55	-42.36	93	49.24	198.30
+26°45'	25	-56.67	-3.48	-53.19	-49.00	-	-	-
+32°10'	30	-61.74	-4.94	-56.80	-52.61	96	47.66	195.09
+37°30'	35	-76.02	-6.74	-69.28	-65.09	99	46.46	192.62

$\alpha$	gross drag lbs.	support drag lbs.	model drag lbs.	fin drag lbs.	$C_D$
0	+ 7.245	+2.598	4.647	+1.754	.919
5	+ 7.379				
10	+ 8.171				
15	+ 9.418				
20	+10.00				
25	+12.654				
30	+14.601				
35	+16.521				

TABLE T

CORING TOOL MODEL (Fin 6)

Type: Regular

Separation: 1 inch

Alignment: +

$\alpha_{bal.}$	$\alpha$	gross moment in lbs.	tare moment in lbs.	net moment in lbs.	adjusted moment in lbs.	temp. °F	cm. H <sub>2</sub> O	speed m.p.h.
+ 15°	0	- 1.21	-	- 1.21	0	94	48.49	196.78
+ 5°10'	5	- 1.60	- .17	- 1.43	- .22	-	-	-
+10°10'	10	-11.81	- .64	-11.17	- 9.96	99	47.88	195.54
+15°10'	15	-25.82	-1.29	-24.53	-23.32	-	-	-
+20°10'	20	-34.45	-2.31	-32.14	-30.93	102	47.19	194.13
+25°15'	25	-43.19	-3.62	-39.57	-38.36	104	-	-
+30°10'	30	-	-	-	-	-	-	-
+35°10'	35	-	-	-	-	-	-	-

$\alpha$	gross drag lbs.	support drag lbs.	model drag lbs.	fin drag lbs.	$C_D$
0	+14.246	+2.598	+11.658	+8.765	2.439
5	+14.077				
10	+14.007				
15	+14.259				
20	+15.211				
25	+16.476				
30	-				
35	-				

TABLE U

CORING TOOL MODEL (Fin 6)

Type: Reversed

Separation: 1.25 inch

Alignment: +

$\alpha_{bal.}$	$\alpha$	gross moment in lbs.	tare moment in lbs.	net moment in lbs.	adjusted moment in lbs.	temp. °F	cm. $H_2O$	speed m.p.h.
+ 30°	0	- 1.94	-	- 1.94	0	82	49.27	198.36
+ 5°40'	5	-16.16	- .09	-16.07	-14.13	-	-	-
+10°55'	10	-30.66	- .61	-30.05	-28.11	89	48.22	196.23
+16°15'	15	-43.89	-1.41	-42.48	-40.54	-	-	-
+21°30'	20	-54.48	-2.56	-51.92	-49.98	93	47.17	194.09
+26°45'	25	-63.36	-4.06	-59.30	-57.36	-	-	-
+32°10'	30	-69.55	-5.96	-63.59	-61.65	96	46.21	192.10
+37°30'	35	-83.70	-7.97	-75.73	-73.79	99	-	-

$\alpha$	gross drag lbs.	support drag lbs.	model drag lbs.	fin drag lbs.	$C_D$
0	+14.769	+2.598	+12.171	+9.278	2.506
5	+15.128				
10	+14.872				
15	+15.093				
20	+15.991				
25	+16.945				
30	+17.976				
35	+19.175				

TABLE V

## CORING TOOL MODEL (Fin 6)

Type: Modified

Separation: 2 inch

Alignment: +

$\alpha_{bal.}$	$\alpha C$	gross moment in lbs.	tare moment in lbs.	net moment in lbs.	adjusted moment in lbs.	temp. °F	cm. H <sub>2</sub> O	speed m.p.h.
+ 30°	0	- 1.81	-	- 1.81	0	94	48.67	197.15
+ 5°40'	5	- 6.571	- .12	- 6.451	- 4.64	-	-	-
+10°55'	10	-15.22	- .63	-14.59	-12.78	98	48.14	196.07
+16°15'	15	-	-1.39	-	-	-	-	-
+21°30'	20	-	-2.49	-	-	-	-	-
+26°45'	25	-	-3.89	-	-	-	-	-
+32°10'	30	-	-5.75	-	-	-	-	-
+37°30'	35	-	-7.72	-	-	-	-	-

Note: Test aborted after  $\alpha C = 10$  degrees due to unpromising results

$\alpha C$	gross drag lbs.	support drag lbs.	model drag lbs.	fin drag lbs.	$C_D$
0	+9.262	+2.598	+6.664	+3.771	1.388
5	+9.375				
10	+9.611				
15	-				
20	-				
25	-				
30	-				
35	-				

TABLE W

$\infty$	cm $H_2O$	speed fps	$R_e$ $\times 10^{-5}$		gross drag lbs	$C_D$		gross drag lbs	$C_D$
without fins									
0	5	92.68	1.370		.855	1.735		.824	1.672
0	10	131.07	1.938		1.275	1.293		1.267	1.285
0	15	160.53	2.374		1.696	1.147		1.738	1.175
0	20	185.36	2.742		2.161	1.096		2.287	1.160
0	25	207.25	3.065		2.751	1.116		2.910	1.180
0	30	227.03	3.357		3.352	1.133		3.583	1.211
0	35	245.22	3.626		4.030	1.168		4.243	1.230
0	40	262.15	3.877		4.646	1.178		4.910	1.245
0	45	278.05	4.112		5.291	1.193		5.624	1.268
0	50	293.09	4.334		5.950	1.207		6.312	1.280

INITIAL DISTRIBUTION LIST

	No. Copies
1. Defense Documentation Center Cameron Station Alexandria, Virginia 22314	20
2. Library Naval Postgraduate School Monterey, California 93940	2
3. Department of Oceanography (Code 58) Naval Postgraduate School Monterey, California 93940	3
4. Prof. R. J. Smith Department of Oceanography Naval Postgraduate School Monterey, California 93940	4
5. LT David C. Honhart, USN Class 27, U. S. Naval Destroyer School Newport, Rhode Island 02840	3
6. Naval Weather Service Command Washington Navy Yard Washington, D. C. 20390	1
7. Prof. D. C. Wooten Department of Aeronautics Naval Postgraduate School Monterey, California 93940	1
8. Prof. R. S. Andrews Department of Oceanography Naval Postgraduate School Monterey, California 93940	1
9. LT Ronald A. Erchul, USN College of Engineering Department of Oceanographic Engineering University of Rhode Island Kingston, R. I. 02881	1
10. LCDR Ernest T. Young, USN USS HARDHEAD (SS 365) FPO New York, 09501	1
11. Commanding Officer Fleet Numerical Weather Central Naval Postgraduate School Monterey, California 93940	1

	No. Copies
12. Superintendent Naval Academy Annapolis, Maryland 21402	1
13. Commanding Officer and Director Navy Electronics Laboratory Attn: Code 2230 San Diego, California 92152	1
14. Director, Naval Research Laboratory Attn: Tech. Services Info. Officer Washington, D. C. 20390	1
15. Department of Meteorology (Code 51) Naval Postgraduate School Monterey, California 93940	1
16. Oceanographer of the Navy The Madison Building 732 N. Washington Street Alexandria, Virginia 22314	1
17. Naval Oceanographic Office Attn: Library Washington, D. C. 20390	1
18. National Oceanographic Data Center Washington, D. C. 20390	1
19. Director, Coast & Geodetic Survey Department of Commerce Attn: Office of Oceanography Washington, D. C. 20235	1
20. Director, Maury Center for Ocean Studies Naval Research Laboratory Washington, D. C. 20390	1
21. Office of Naval Research Department of the Navy Attn: Undersea Warfare (Code 466) Washington, D. C. 20360	1
22. Office of Naval Research Department of the Navy Attn: Geophysics Branch (Code 416) Washington, D. C. 20360	1

Unclassified

Security Classification

DOCUMENT CONTROL DATA - R & D

Security classification of title, body of abstract and indexing annotation must be entered when the overall report is classified

1. ORIGINATING ACTIVITY (Corporate author) Naval Postgraduate School Monterey, California 93940	2a. REPORT SECURITY CLASSIFICATION Unclassified	
3. REPORT TITLE Stabilizing Fins for Underwater Coring Tools		
4. DESCRIPTIVE NOTES (Type of report and, inclusive dates) Thesis, December 1968		
5. AUTHOR(S) (First name, middle initial, last name) David Crosby Honhart		
6. REPORT DATE December 1968	7a. TOTAL NO. OF PAGES 72	7b. NO. OF REFS 7
8a. CONTRACT OR GRANT NO.	9a. ORIGINATOR'S REPORT NUMBER(S)	
b. PROJECT NO. N/A	N/A	
c.	9b. OTHER REPORT NO(S) (Any other numbers that may be assigned this report)	
d.		
10. DISTRIBUTION STATEMENT Distribution of this document is unlimited.		
11. SUPPLEMENTARY NOTES	12. SPONSORING MILITARY ACTIVITY Naval Postgraduate School Monterey, California 93940	

13. ABSTRACT

It is essential that the force vector of the weight of a coring tool act along a line that is parallel to the longitudinal axis of the core barrel. Such an alignment enables corers to obtain deeper, less disturbed core samples. The probability of bending the core barrel is furthermore greatly reduced. A fin assembly that provides the maximum righting moment for one shape of coring tool does not necessarily provide the maximum moment for a different shape. The optimum fin design is determined by testing. A fin assembly for a particular coring tool has been devised which reduces the probability of the force vector not acting parallel to the longitudinal axis. The optimum design is a vane-shroud fin assembly. The shape of the shroud is conical. Slotting the shroud by removing longitudinal strips improves the righting capability at higher angles of deviation, but is slightly inferior to the full shroud at lesser angles.

Unclassified

Security Classification

1.4 KEY WORDS	LINK A		LINK B		LINK C	
	ROLE	WT	ROLE	WT	ROLE	WT
Stabilizing Fins for Underwater Coring Tools						
Fin Assemblies for underwater coring Tools						
Coring Tool Fin Assemblies						

DD FORM 1473 (BACK)

1 NOV 65  
1/N 0101-F07-6921











thesH729  
Stabilizing fins for underwater coring t



3 2768 002 06964 3  
DUDLEY KNOX LIBRARY